

# 磁化中性子星への超臨界降着によるアウトフロー； 駆動機構と温度について

Outflows driven by super-critical accretion flows  
on to magnetized neutron stars ;  
Driven mechanisms and temperatures

---

Akihiro Inoue (University of Tsukuba)

Ken Ohsuga (University of Tsukuba)

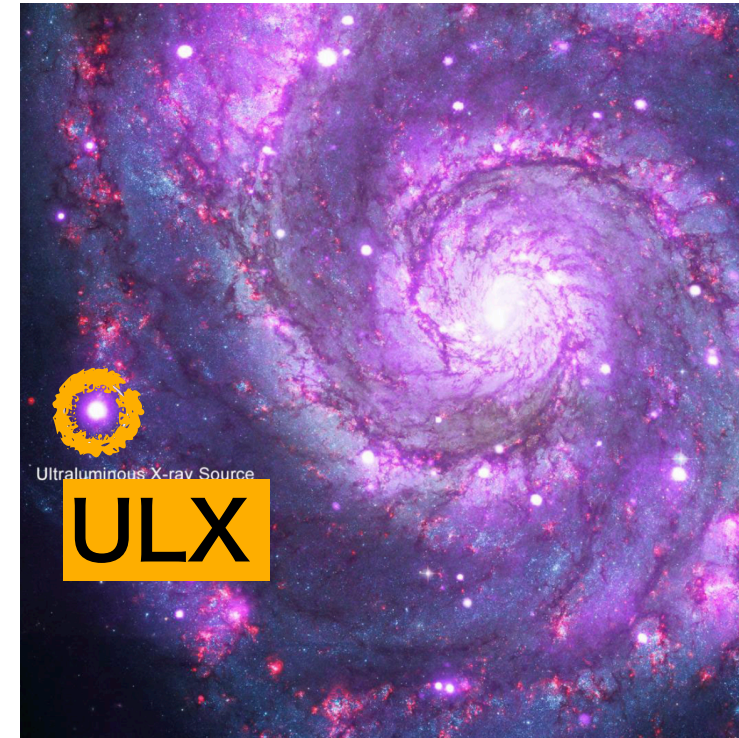
Hiroyuki R. Takahashi (Komazawa University)

Yuta Asahina (University of Tsukuba)

Tomohisa Kawashima (University of Tokyo)

# Ultra-Luminous X-ray Sources (ULXs)

Off-nuclear, compact, X-ray sources of which X-ray luminosity exceeds the Eddington luminosity for the stellar mass black holes,  $\sim 10^{39}$  erg s<sup>-1</sup>.



©NASA

It has been thought to be either

- **stellar mass black hole + Supercritical accretion**  
(King+2001, Watarai+2001, . . .)

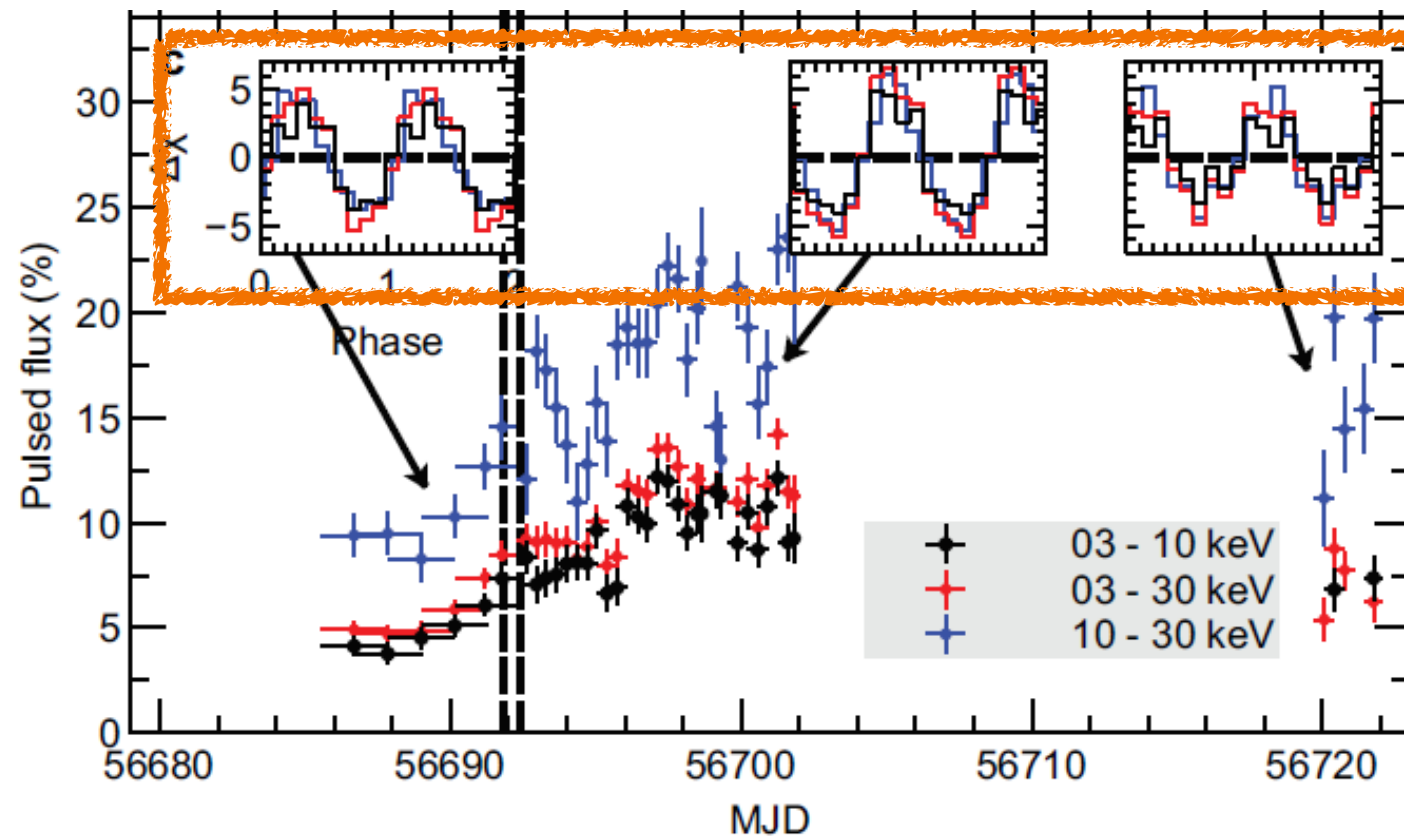
or

- **Intermediate-mass black hole + Sub-Eddington accretion**  
(Colbert & Mushotzky 1999, Makishima+2000, . . .)

However, it has not been settled yet . . .

# Ultra-Luminous X-ray Pulsar (ULX Pulsar)

The central objects of some ULXs turned out to be neutron stars (NSs) since recent X-ray observations detected the pulsed emission.



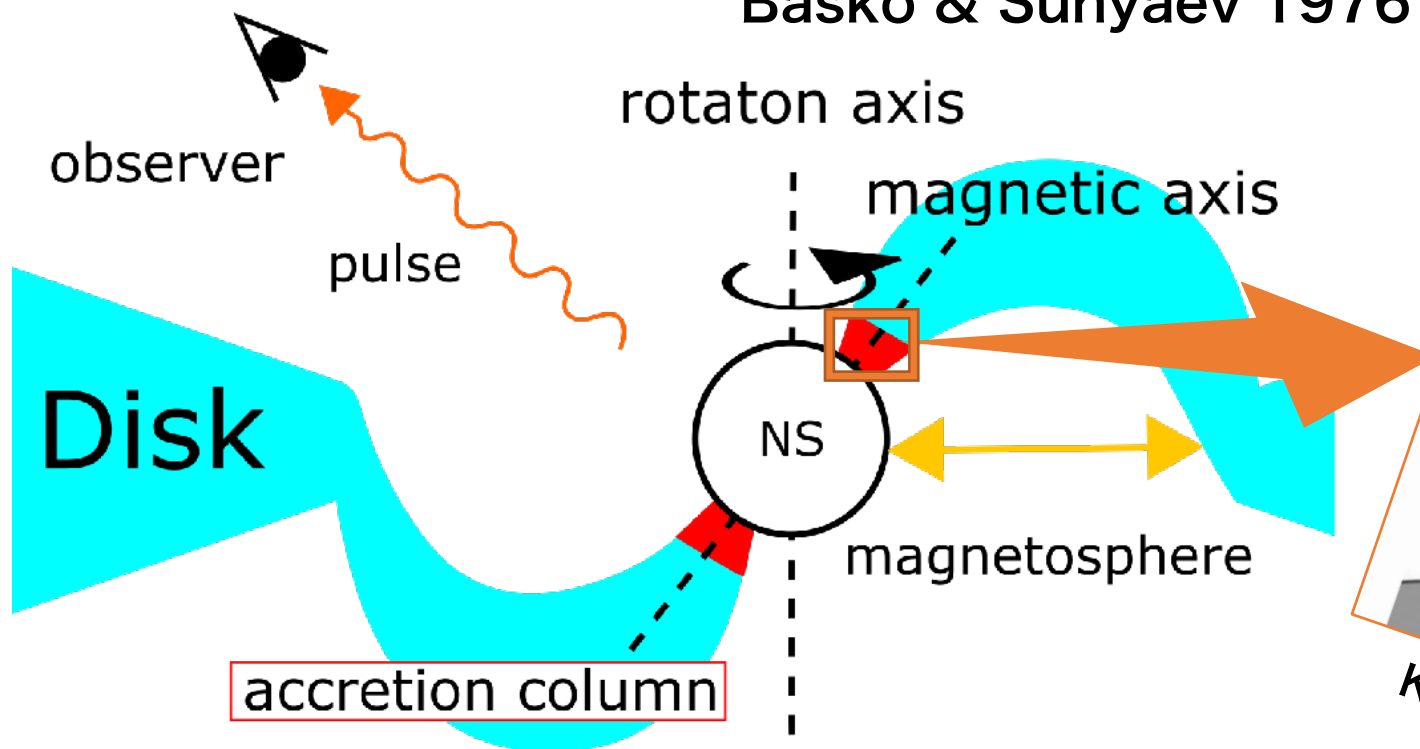
M82 X-2  
Bachetti+2014

- The mass of NSs is  $(1.4 - 3)M_{\odot}$ , and therefore the matter should accrete at the **super-critical rate** where the mass accretion rate exceeds the Eddington accretion rate,  $\dot{M}_{\text{Edd}} \sim 10^{17} \text{ g s}^{-1}$ .
- There are still debates on the magnetic field strength in ULX Pulsars, from  $10^{10} \text{ G}$  (see e.g., King + 2017) to  $10^{15} \text{ G}$  (see e.g., Mushtukov+2015).

# The theoretical model of ULX Pulsars

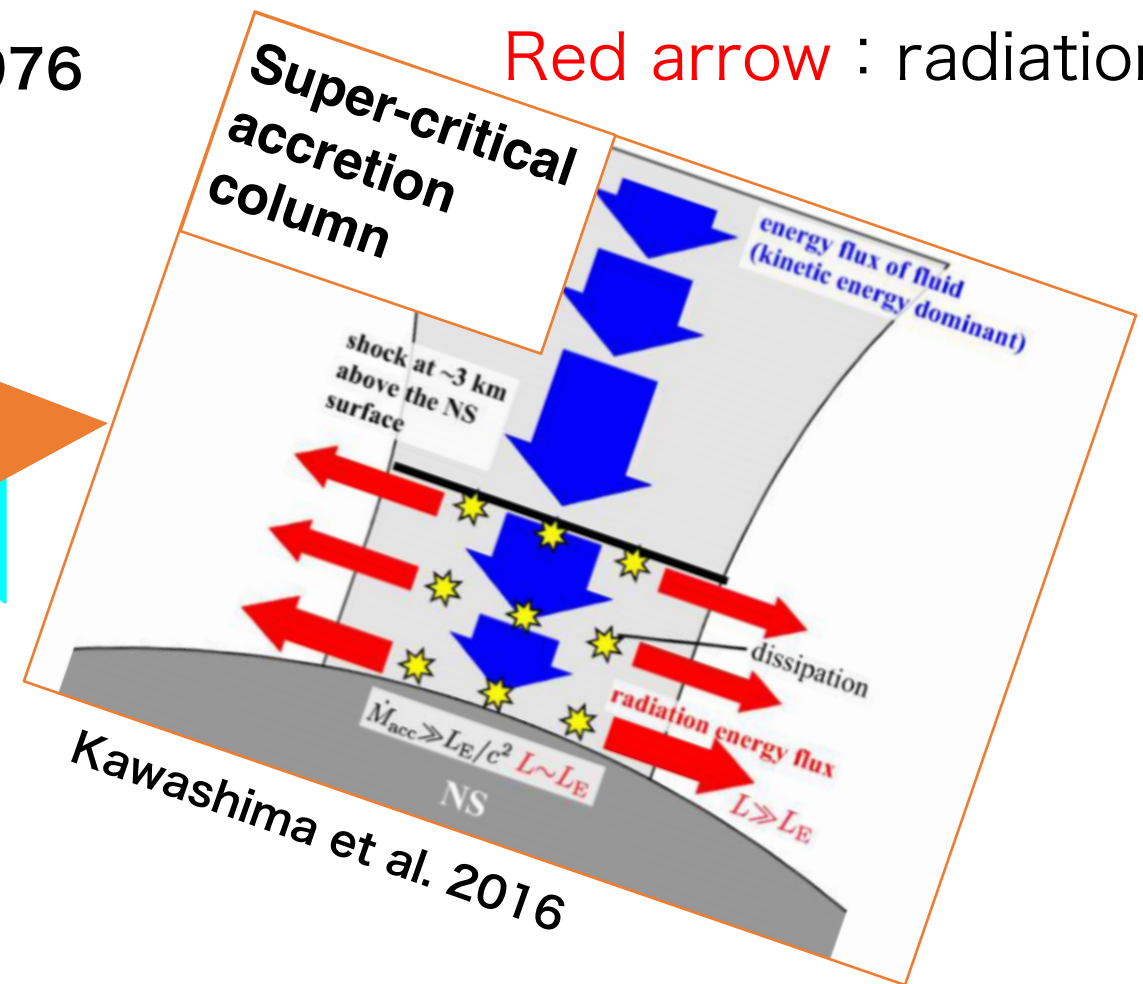
## Super-critical column accretion

Basko & Sunyaev 1976

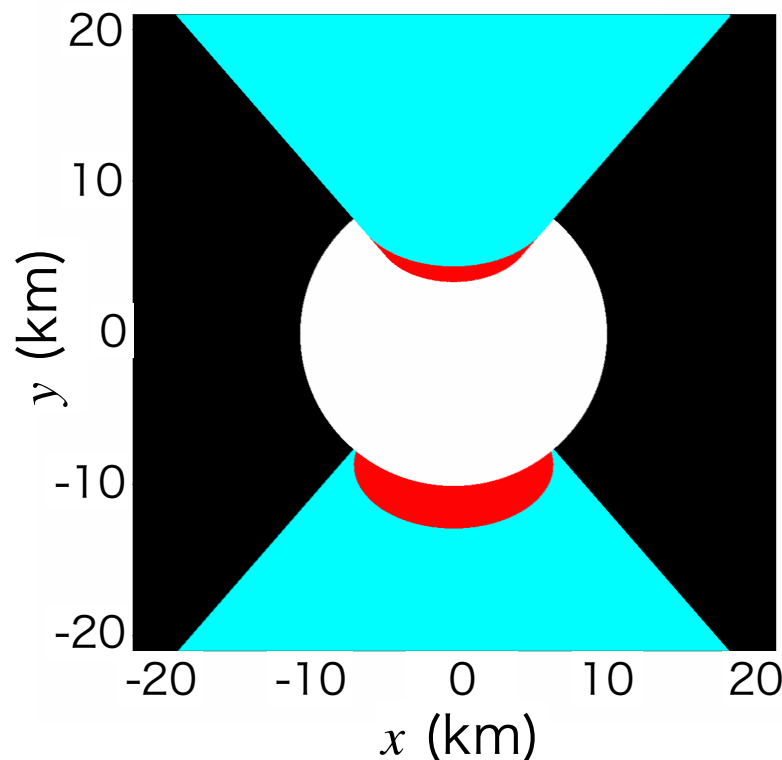


Blue arrow : gas motion

Red arrow : radiation flow



Schematic view

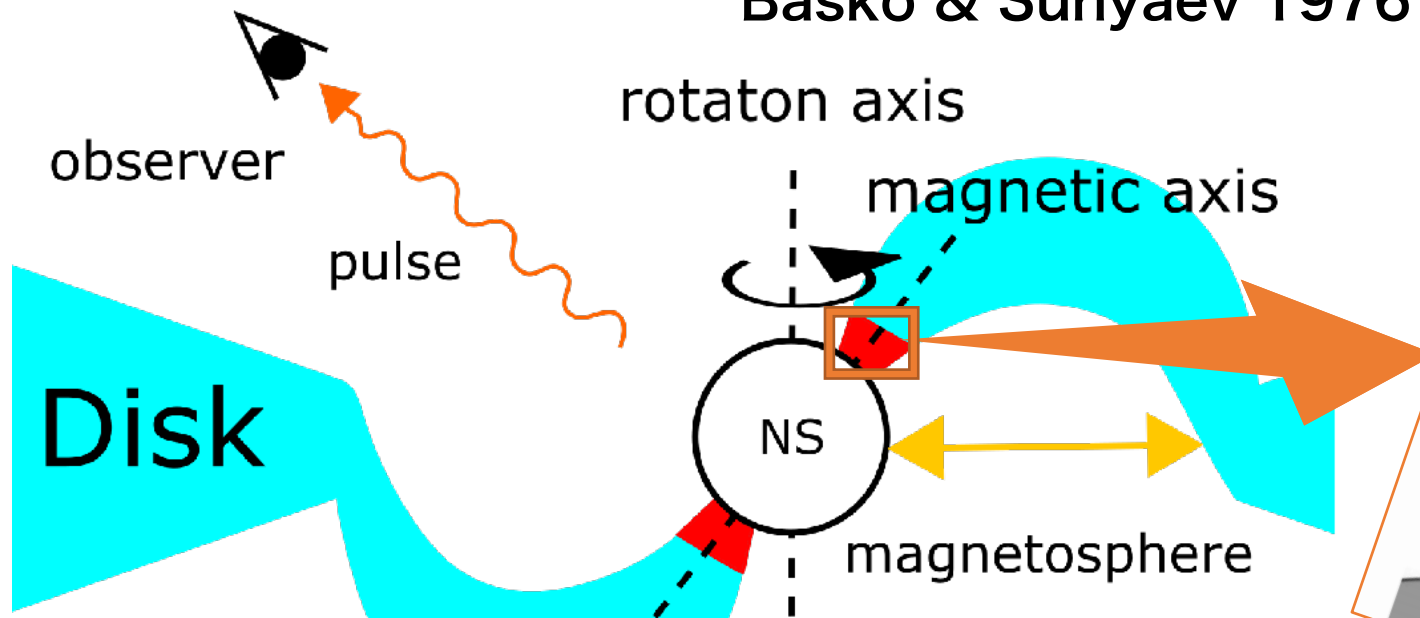


- The side wall of the column near the NS is the main radiation source ( $>$ Eddington luminosity).
- If the magnetic axis is misaligned with the rotation axis, observed luminosity periodically changes via precession of the column.

# The theoretical model of ULX Pulsars

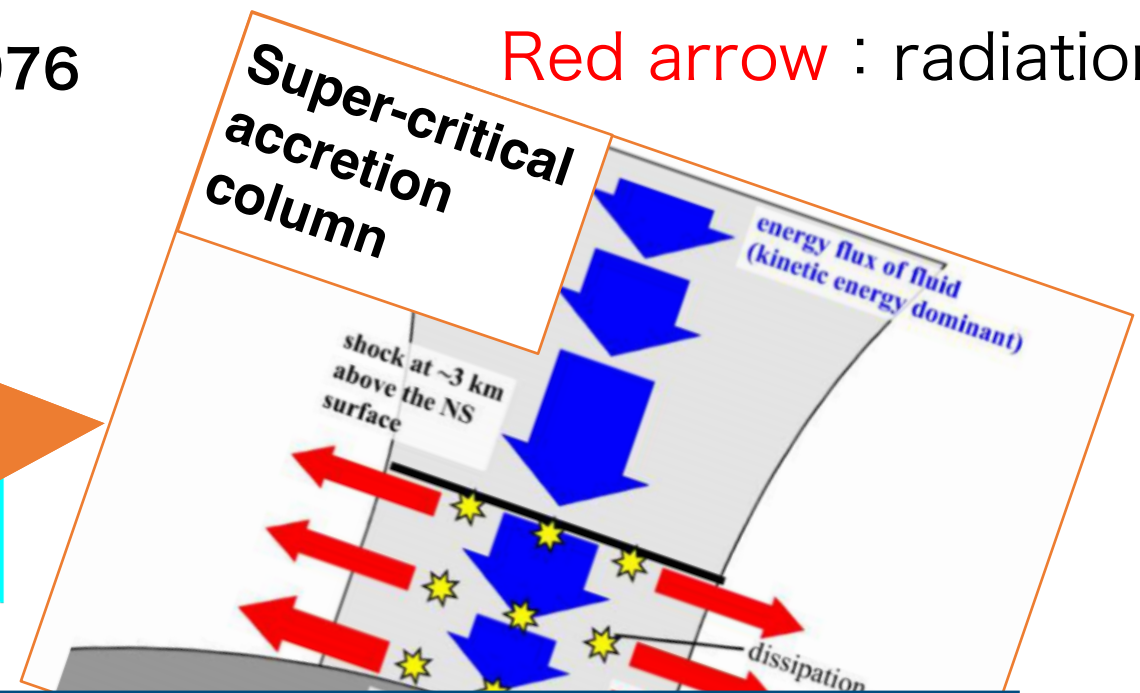
## Super-critical column accretion

Basko & Sunyaev 1976

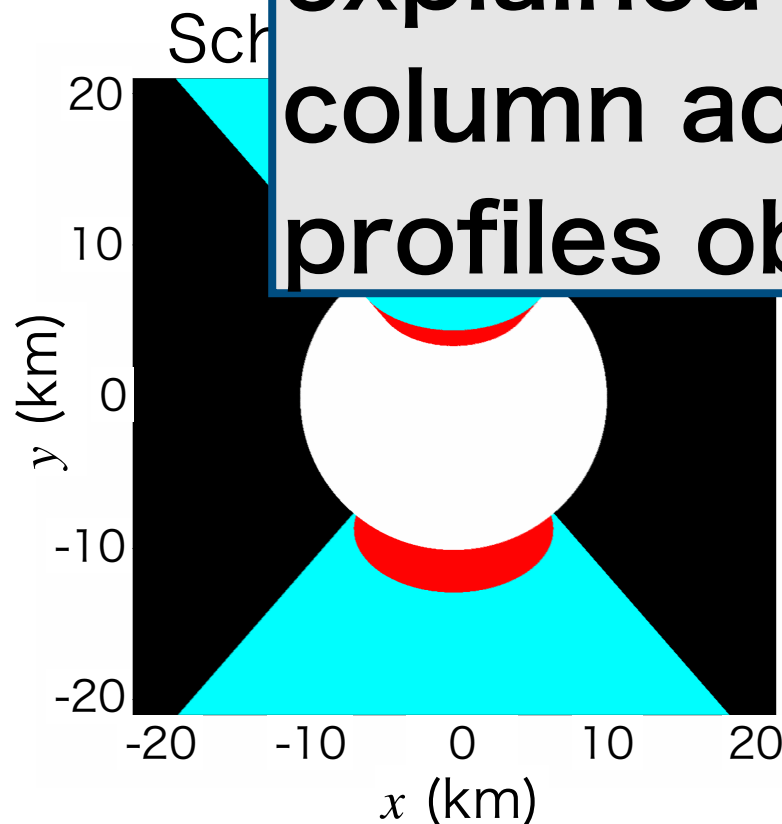


Blue arrow : gas motion

Red arrow : radiation flow



ad However, it has not been completely explained yet whether the super-critical column accretion can explain pulse profiles observed in ULX Pulsars or not.

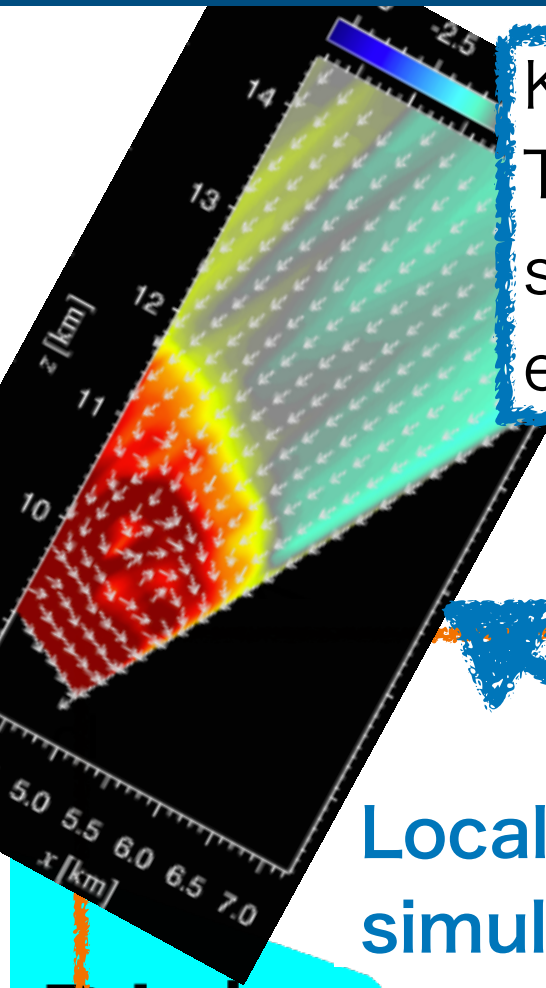


- S is the main radiation source ( $> E_{\text{Eddington}}$  luminosity).
- If the magnetic axis is misaligned with the rotation axis, observed luminosity periodically changes via precession of the column.

# Hydrodynamical Simulations around magnetized NSs

Kawashima+2016

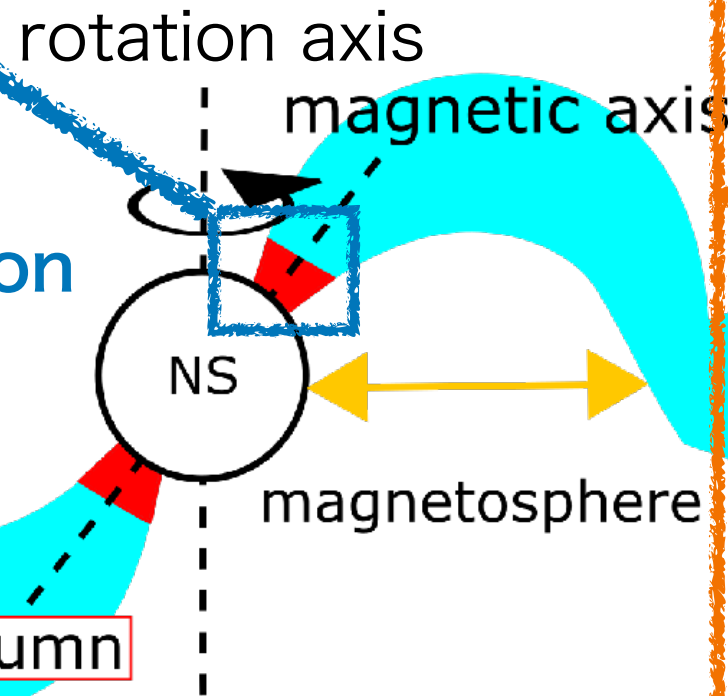
They showed that the luminosity of side walls of the column near the NS exceeds the Eddington luminosity.



Global simulation

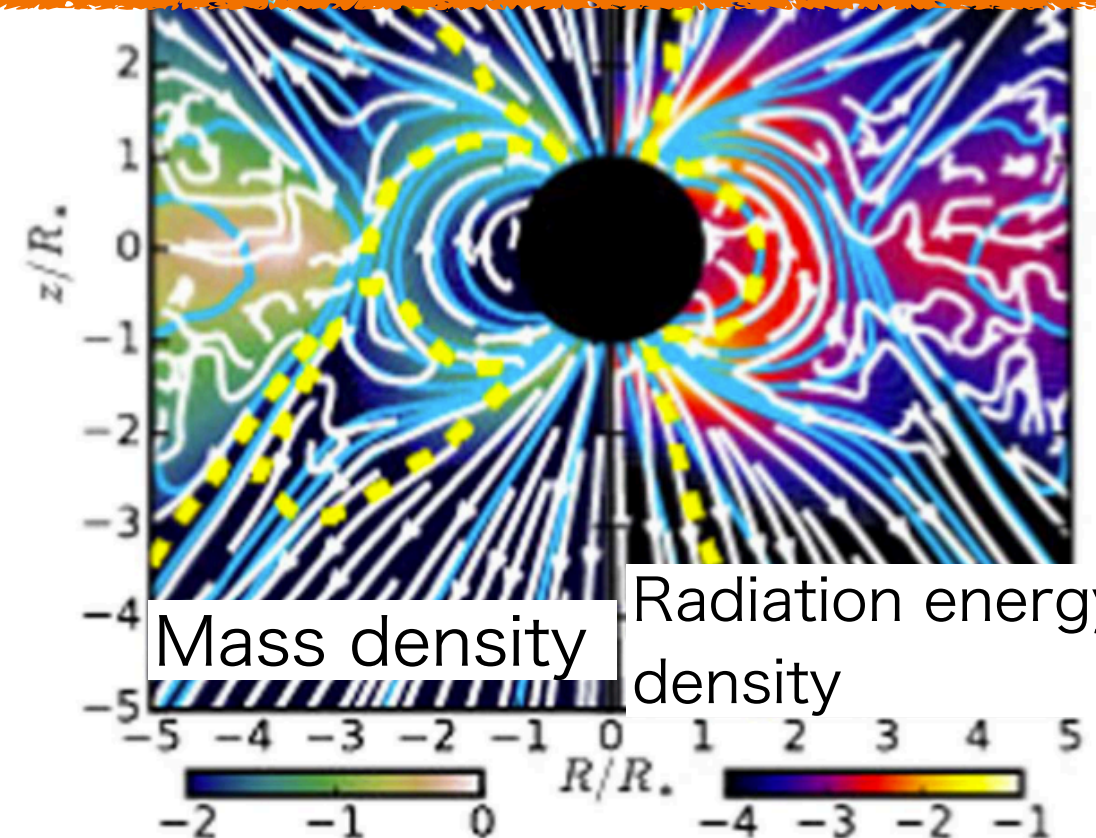
Local simulation

Disk



Takahashi & Ohsuga 2017

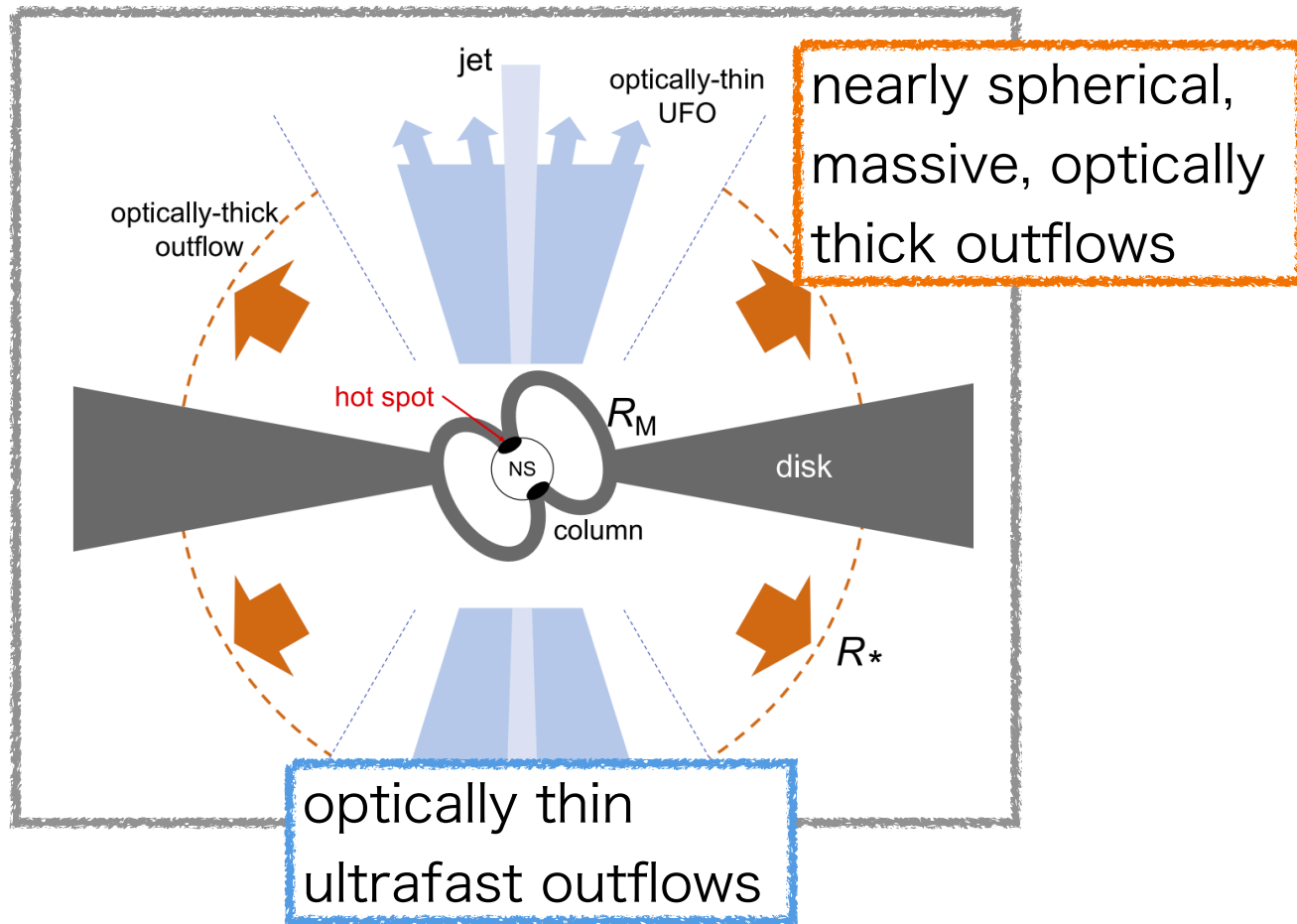
They showed that the supercritical accretion disk is truncated by the dipole magnetic field of the NS, and is formed the accretion columns on the magnetic poles.



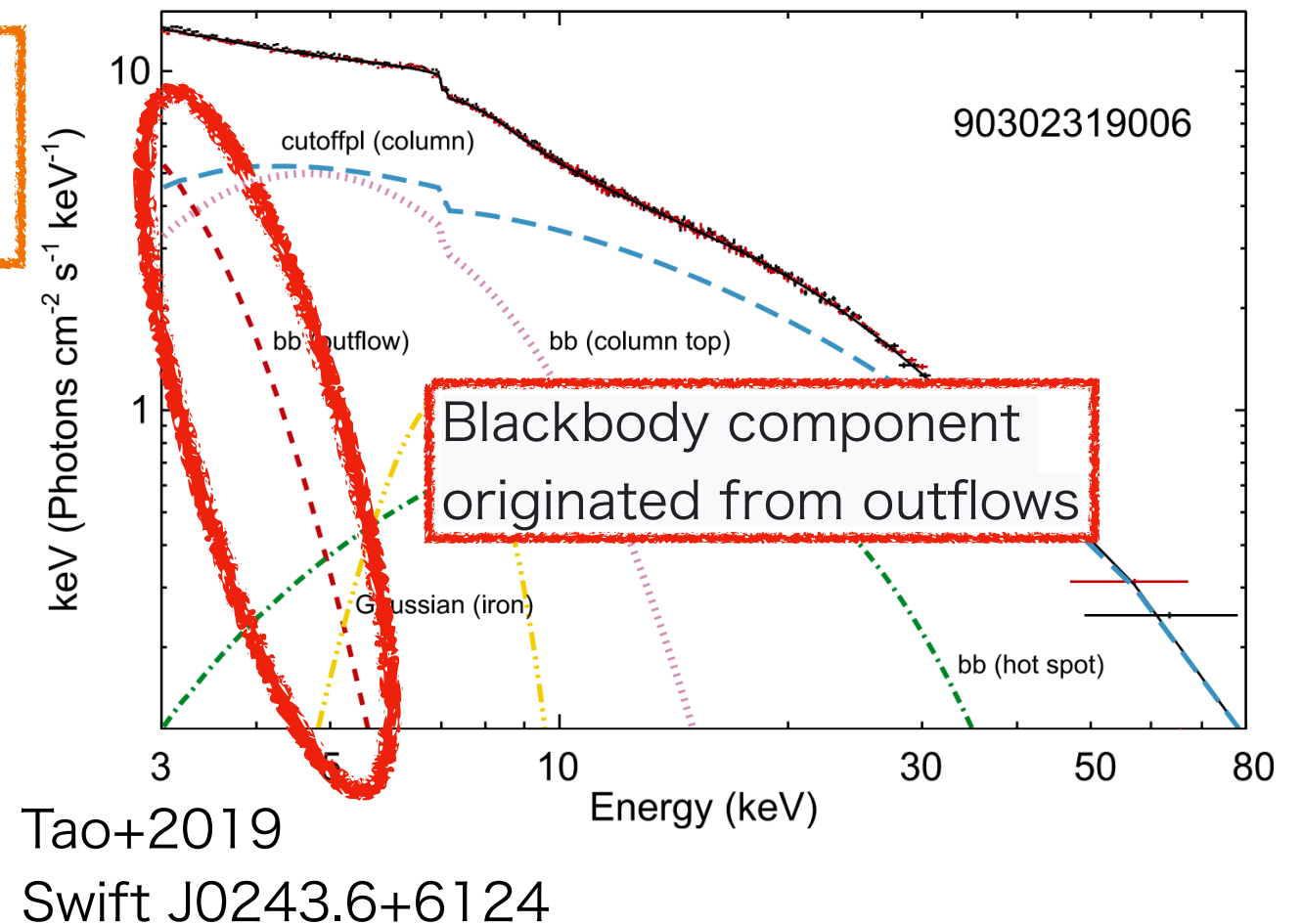
The magnetic field strength of NSs and the mass accretion rate determine the magnetospheric structure.

# Outflows driven by super-critical accretions

Schematic view of outflows



Radiation spectrum of ULXP



## Thermal emission

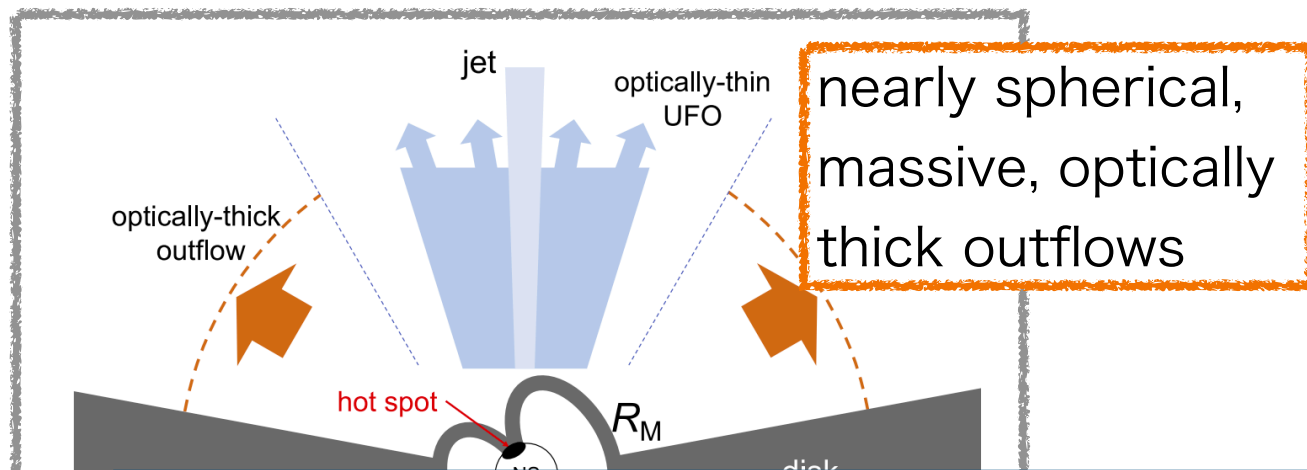
Blackbody temperature : 0.5keV , Blackbody radius : 100-500km

## Blueshifted (0.1c-0.2c) absorption line

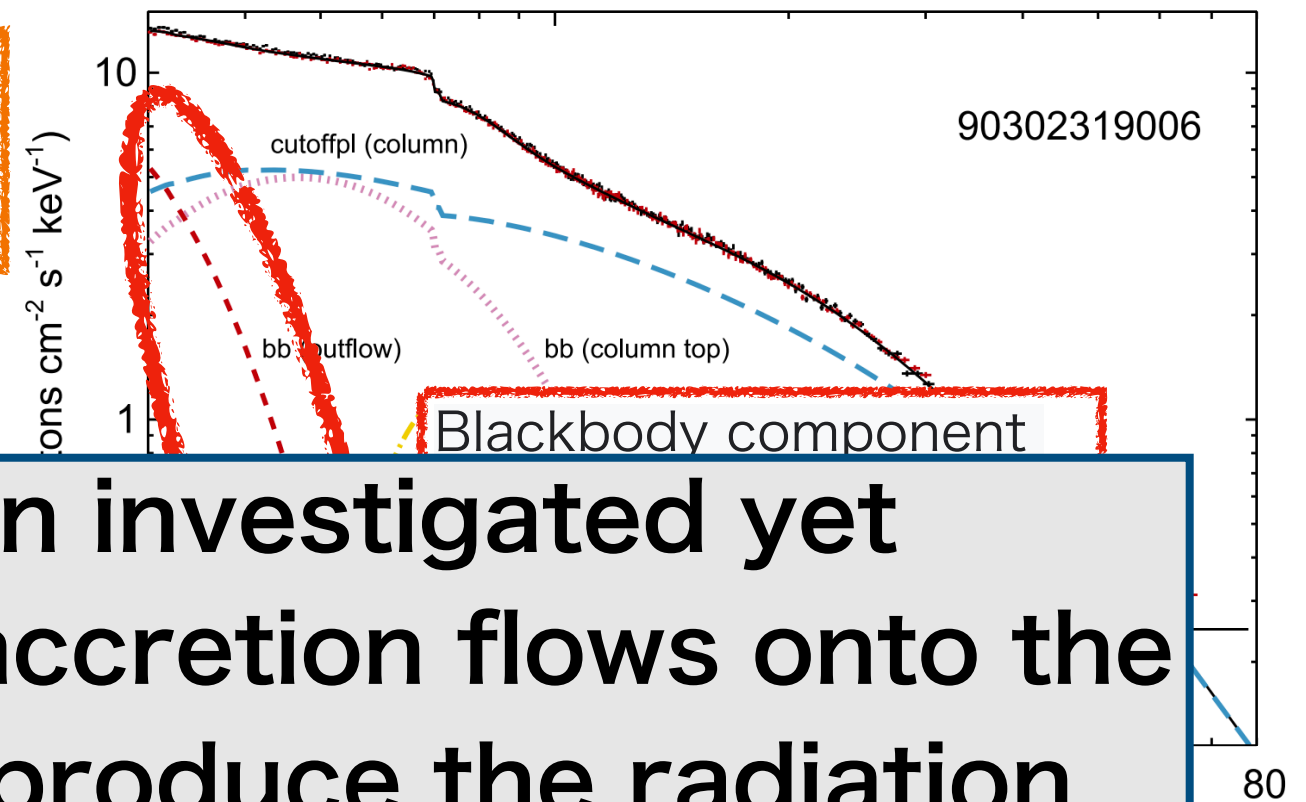
(See also, Kosec et al. 2018, Pinto et al. 2016, 2017; Walton et al. 2016)

# Outflows driven by super-critical accretions

Schematic view of outflows



Radiation spectrum of ULXP



However, it has not been investigated yet whether super-critical accretion flows onto the magnetized NSs can reproduce the radiation spectrum and the outflow velocity observed in ULX Pulsars or not.

**Thermal emission**

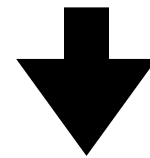
Blackbody temperature : 0.5keV , Blackbody radius : 100-500km

**Blueshifted (0.1c-0.2c) absorption line**

(See also, Kosec et al. 2018, Pinto et al. 2016, 2017; Walton et al. 2016)

# Questions in ULX Pulsars

- ① Can super-critical column accretion flows explain pulse profiles observed in ULX Pulsars?
- ② Is it possible to reproduce outflow temperatures and outflow velocities observed in ULX pulsars with super-critical accretion flows onto magnetized NSs?



Numerical simulations

## This study

We perform that

- ① radiative transfer simulations using simulation results in Kawashima et al. 2016 to calculate the pulse profile (Inoue et al. 2020).
- ② general relativistic radiation magneto-hydrodynamical simulations to investigate the mechanisms of outflows (but 2D simulation).

These make it possible to limit the physical quantities (mass accretion rate, etc.) that cannot be directly observed as well as to investigate the validity of the theoretical model obtained by numerical simulation.

**Pulse profile calculated  
from super-critical column accretions  
(Inoue et al. 2020)**

# Radiative transfer simulations

The geodesic equation for light (Schwarzschild metric)

$$\frac{d^2}{d\varphi^2} \left( \frac{1}{r} \right) + \frac{1}{r} = \frac{3r_s}{2} \left( \frac{1}{r} \right)^2$$

Light bending effect

Intensity, Isotropic Luminosity

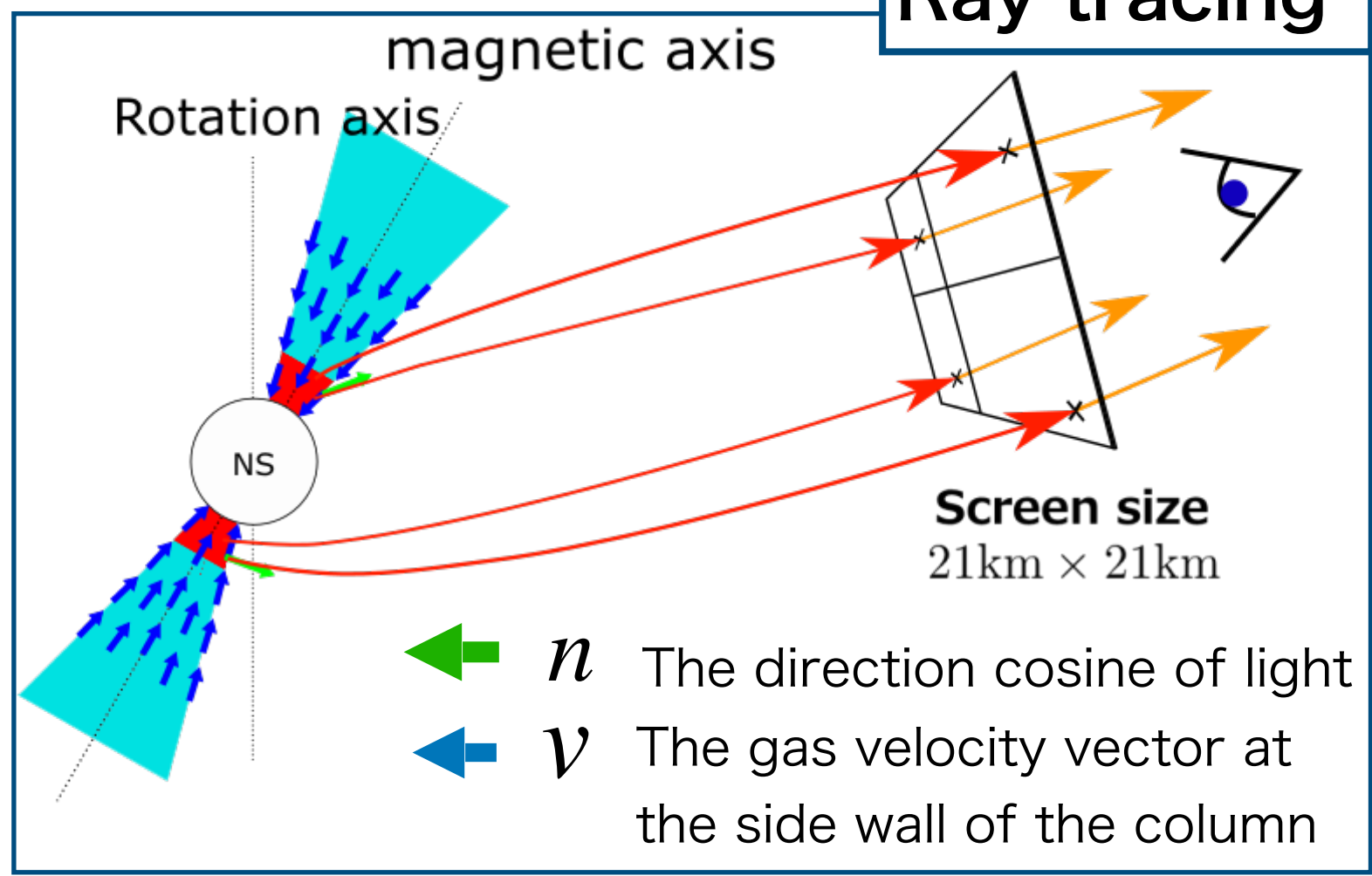
$$I_{\text{obs}} = \frac{B_0}{(1+z)^4}$$

$B_0$  : black body intensity

$$L_{\text{obs}} = 4\pi \sum_i I_{\text{obs}} dA$$

summation for all pixels

## Ray tracing



See Inoue et al. 2020 for detailed conditions

Relativistic Effect

$$1+z = \frac{1}{\sqrt{1-r_s/r}} \left[ \gamma \left( 1 - \frac{\mathbf{v} \cdot \mathbf{n}}{c} \right) \right]$$

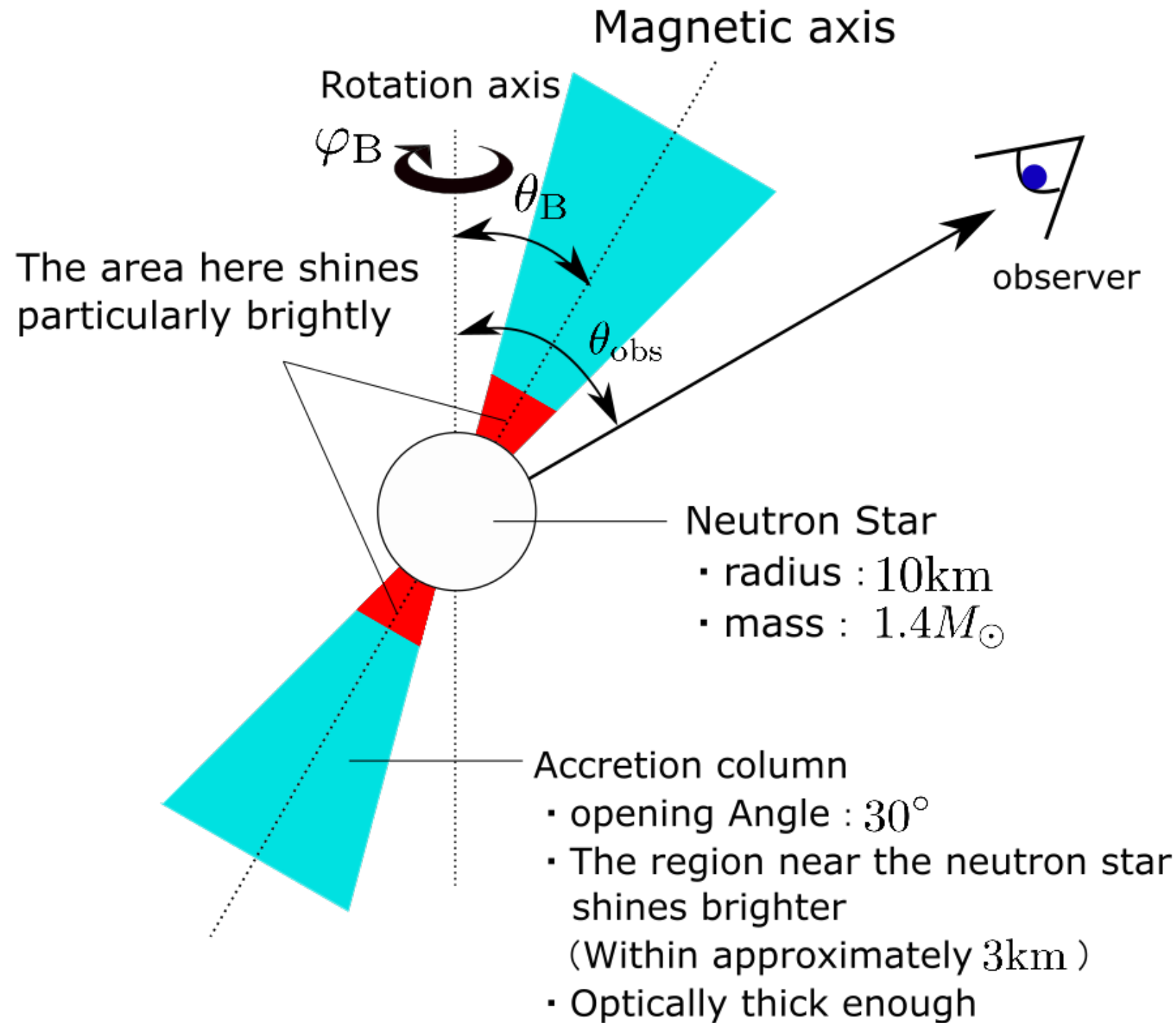
BLACK-HOLE ACCRETION DISK  
S,Kato J,Fukue S,Mineshige(1998)

Gravitational redshift

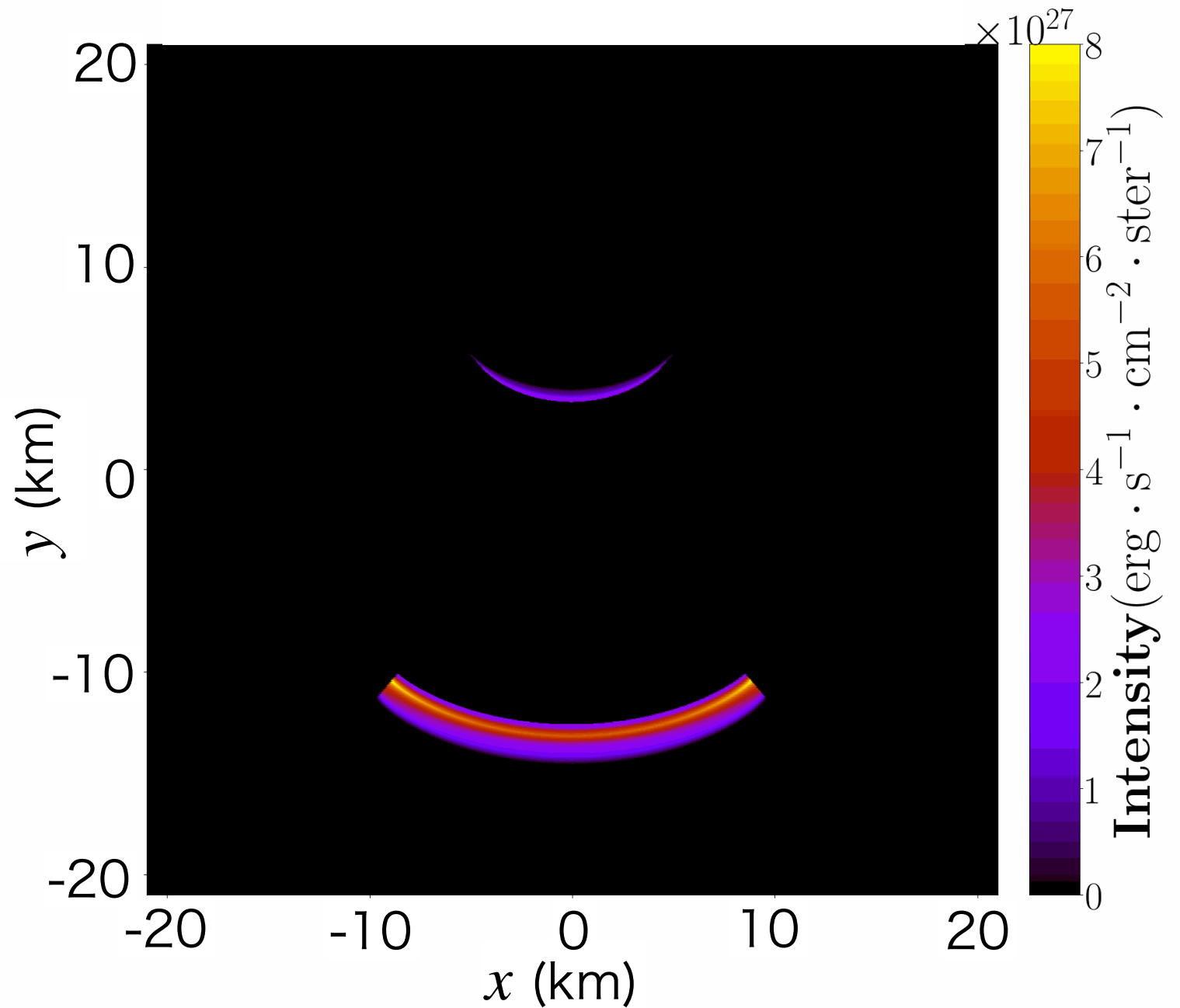
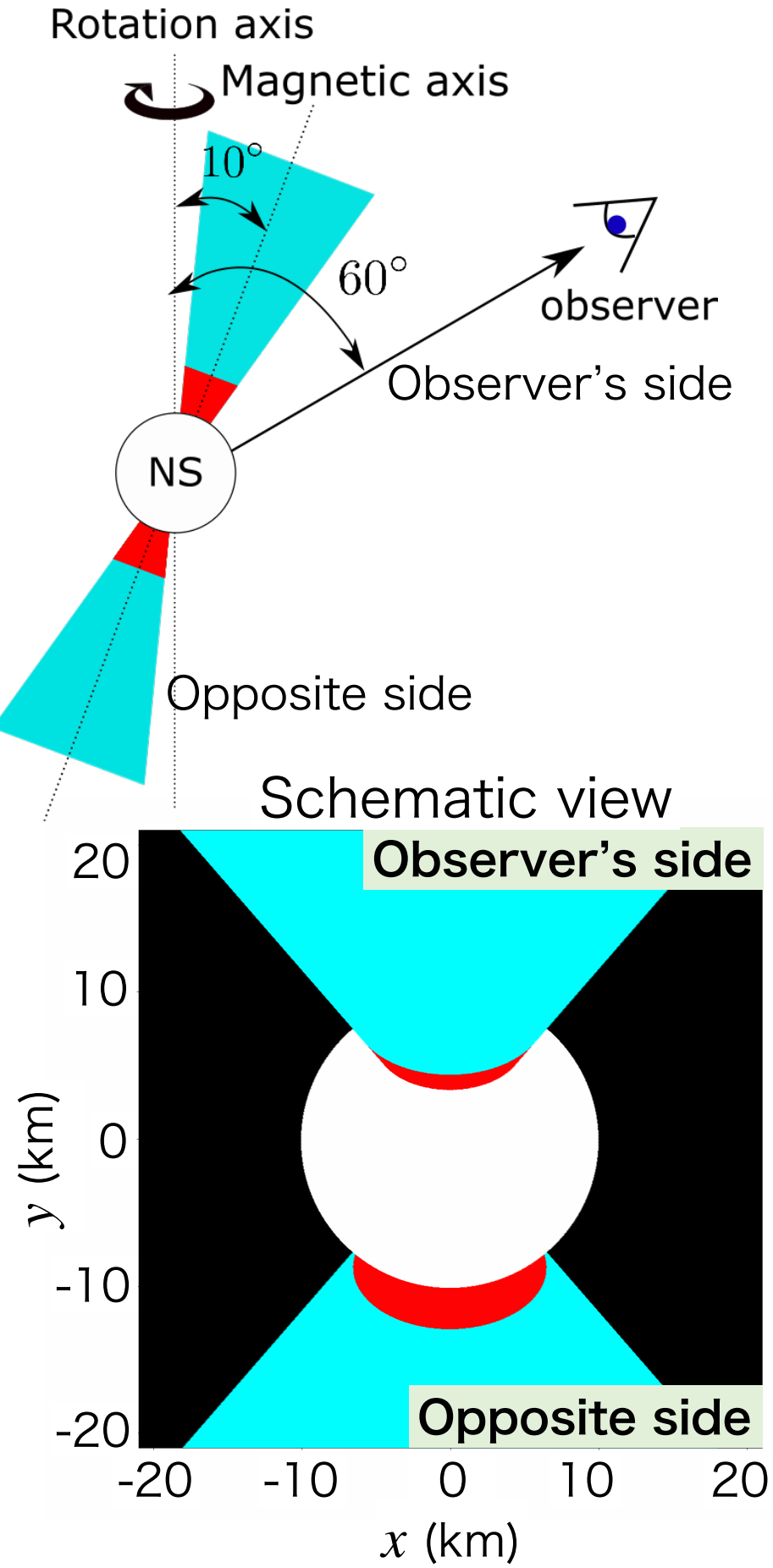
Relativistic doppler effect

# Model and assumptions

- We employ the profiles of the temperature and the velocity obtained by the radiation hydrodynamics simulation (Kawashima et al. 2016).
- The accretion column is steady and axisymmetric with respect to the magnetic axis.
- The column is very optically thick. Thus, the side wall of the column is the photosphere.
- Outside of the accretion columns is almost vacuum (very optically thin).



# Intensity map



- Due to the Doppler effect, the opposite side of the column seems to be bright.
- Opposite side is seen widened because of the light bending (gravitational lensing).

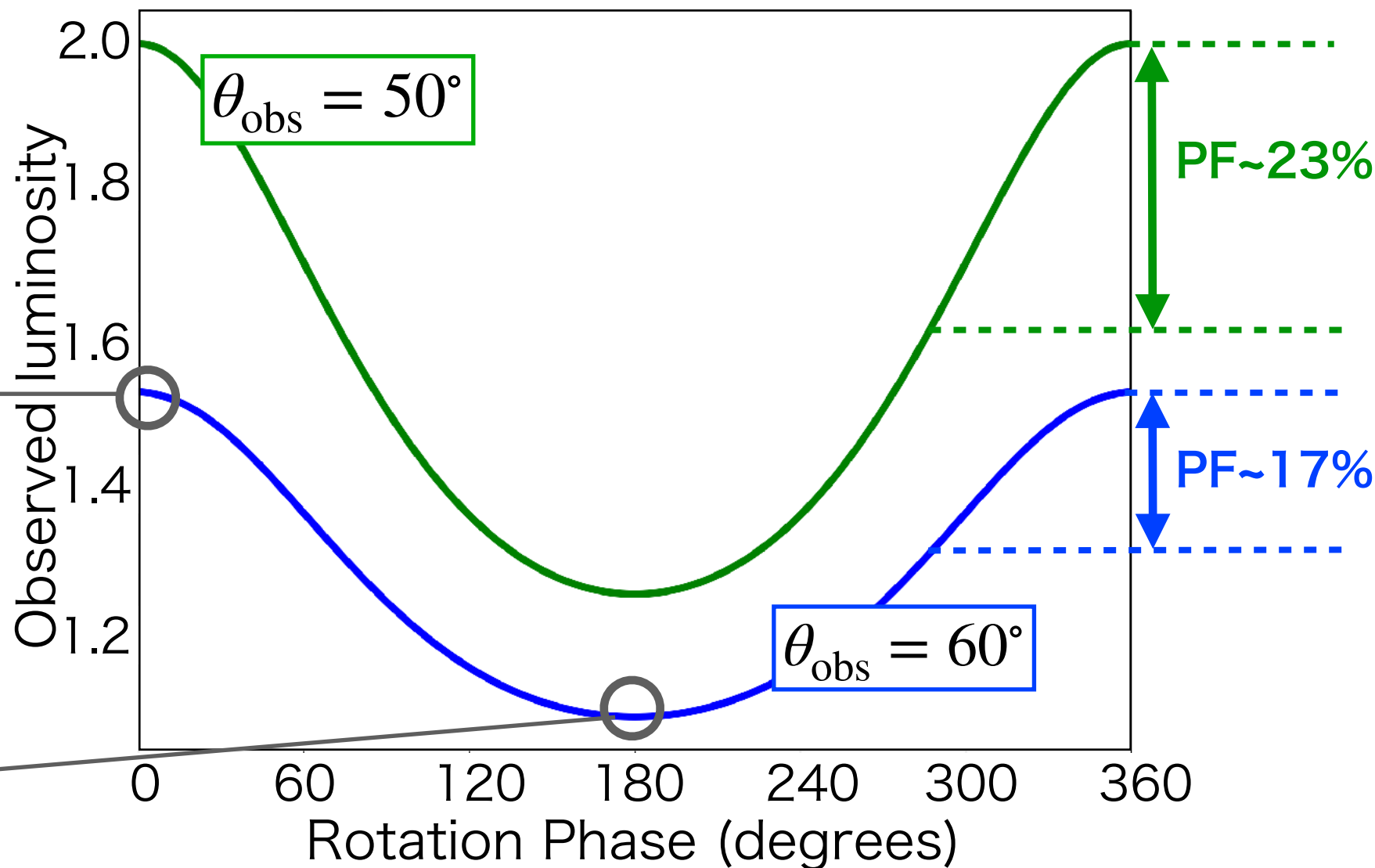
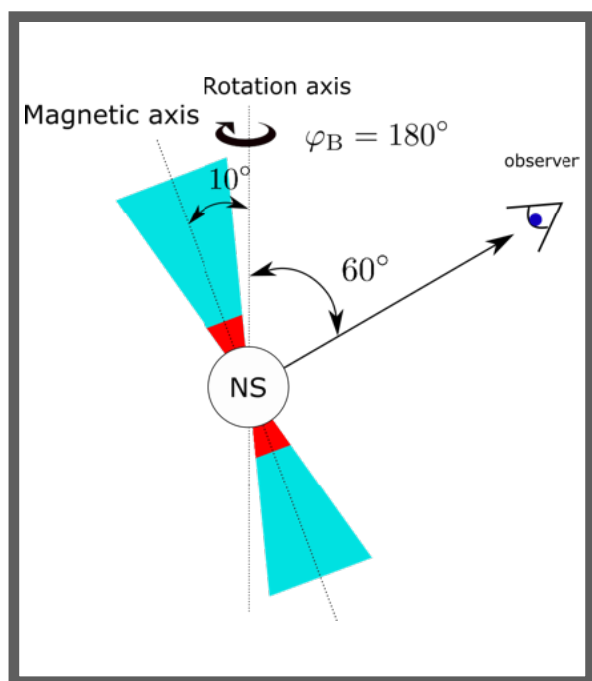
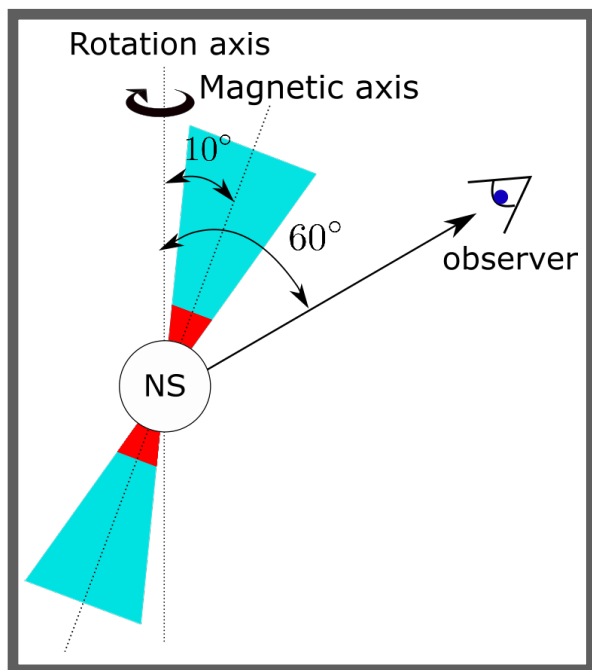
# Pulse profiles and Pulsed fraction (PF)

$$PF \equiv \frac{L_{\text{Max}} - L_{\text{min}}}{L_{\text{Max}} + L_{\text{min}}}$$

$\theta_B$  : The angle of the magnetic axis

$\theta_{\text{obs}}$  : Observer's viewing angle

$\times 10^{40}$  Pulse profile at  $\theta_B = 10^\circ$



- Super-critical column accretion model can exhibit the X-ray pulse via the precession of the column.
- The resulting PF can reach up to 60%.

**Pulse profiles and pulsed fraction obtained in this study are consistent with most observations in ULX Pulsars.**

**Outflow mechanisms in super-critical  
accretion onto magnetized NSs  
(Inoue et al. in prep)**

# GR-RMHD equation

Mass cons.  $\partial_t (\sqrt{-g} \rho u^t) + \partial_i (\sqrt{-g} \rho u^i) = 0$

Gauss law  $\partial_i (\sqrt{-g} B^i) = 0$

Induction eq.  $\partial_t (\sqrt{-g} B^i) = -\partial_j [\sqrt{-g} (b^j u^i - b^i u^j)]$

Energy-momentum cons. for ideal MHD  $\partial_t (\sqrt{-g} T_\nu^t) + \partial_i (\sqrt{-g} T_\nu^i) = \sqrt{-g} T_\lambda^\kappa \Gamma_{\nu\kappa}^\lambda + \boxed{\sqrt{-g} G_\nu}$

Energy-momentum cons. for radiation  $\partial_t (\sqrt{-g} R_\nu^t) + \partial_i (\sqrt{-g} R_\nu^i) = \sqrt{-g} R_\lambda^\kappa \Gamma_{\nu\kappa}^\lambda - \boxed{\sqrt{-g} G_\nu}$

Radiation four force  $G^\mu = -\rho \kappa_{\text{abs}} (R^\mu_\alpha u^\alpha + 4\pi \hat{B} u^\mu) - \rho \kappa_{\text{sca}} (R^\mu_\alpha u^\alpha + R^\alpha_\beta u_\alpha u^\beta u^\mu) + G^\mu_{\text{comp}}$

M1-closure  $R^{\mu\nu} = \frac{4}{3} \bar{E}_R u_R^\mu u_R^\nu + \frac{1}{3} \bar{E}_R g^{\mu\nu}$

Sadowski+ 2013, 2014

$\rho$  mass density,  $u^\mu$  four velocity of the gas  
 $g$  determinant of metric,  $B^i$  magnetic three vector  
 $b^\mu$  covariant magnetic field,  
 $T^{\mu\nu}$  ideal MHD energy-momentum tensor  
 $R^{\mu\nu}$  radiation energy-momentum tensor  
 $\kappa_{\text{abs}}$  free-free, synchrotron opacity  
 $\kappa_{\text{sca}}$  electron scattering,  $\Gamma_{\alpha\beta}^\mu$  Christoffel symbol  
 $G^\mu_{\text{comp}}$  thermal Compton,  $\hat{B}$  Black-body intensity  
 $\bar{E}_R$  radiation energy in radiation rest-frame  
 $u_R^\mu$  four velocity of radiation

The interaction between the MHD and the radiation may be described with this term.

- We use the GR-RMHD code UWABAMI (Takahashi & Ohsuga 2017)
- Schwarzschild Metric are employed.
- The magnetic axis coincides with the rotation axis (Axisymmetric structure).

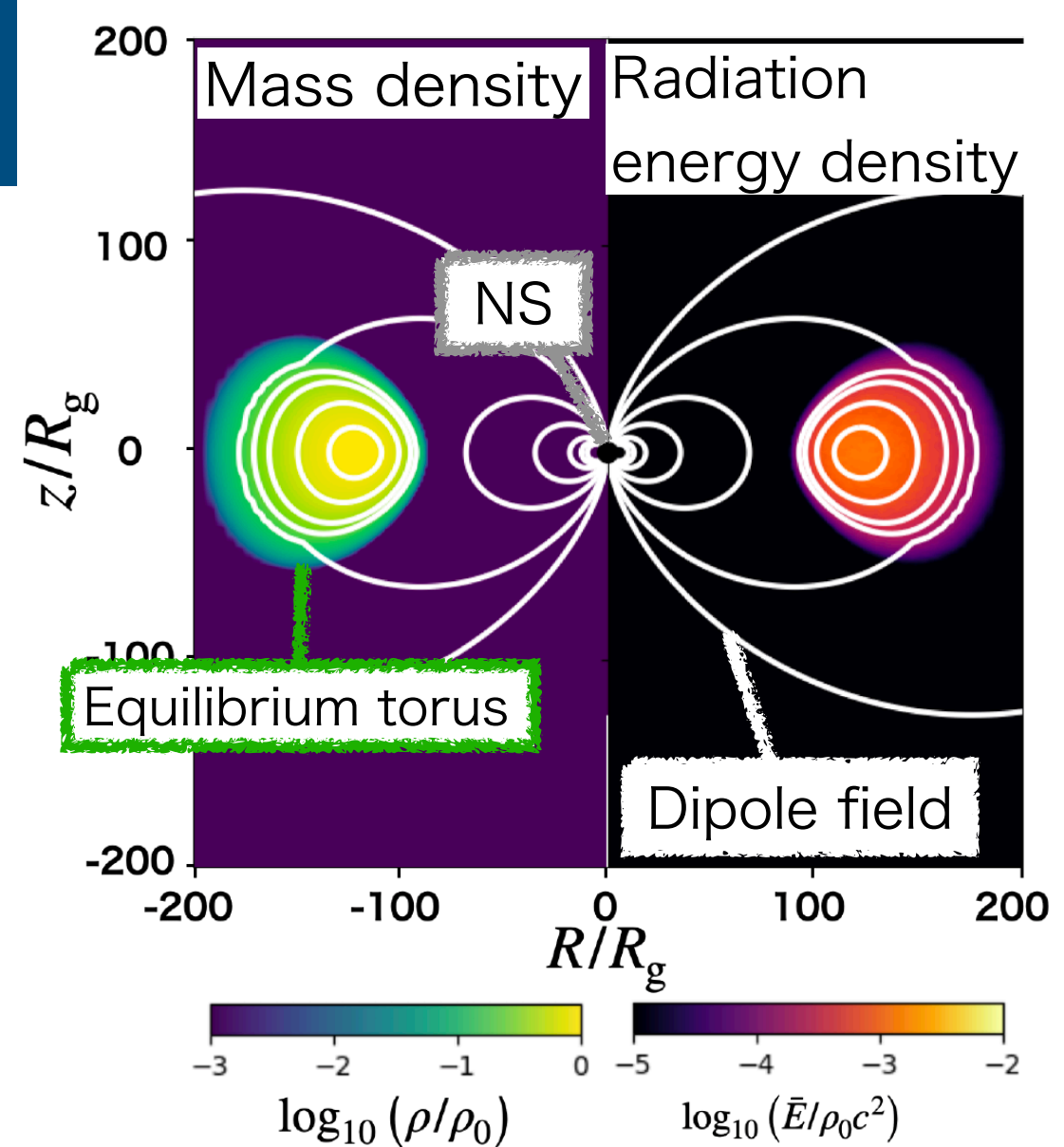
# Set up

Computational domain :  $r = [R_{\text{NS}}, 2800R_{\text{NS}}]$ ,  $\theta = [0, \pi]$

Grid number :  $(N_r, N_\theta, N_\phi) = (450, 300, 1)$

## Neutron Star (NS)

- Mass  $1.4 M_\odot$  • Radius 10km
- magnetic dipole field
- The boundary condition at the NS surface  
Gases are adsorbed on the NS surface  
Radiation fields become isotropic



$R_g \sim 2.1 \text{ km}$

## Equilibrium torus (Fishbone & Moncrief 1976)

- inner edge : 180km • pressure maximum of the torus : 250km
- We set the loop magnetic field in proportion to the density

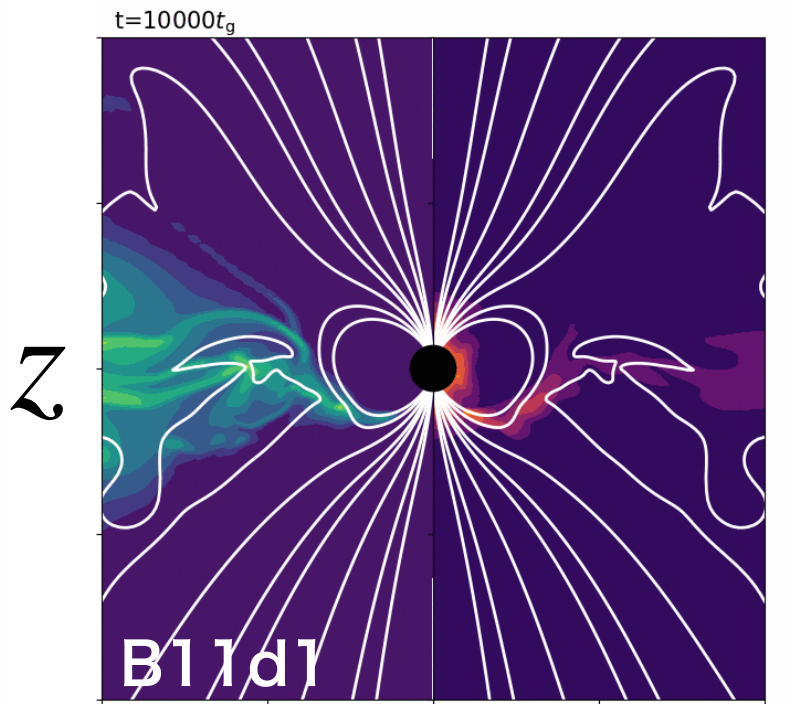
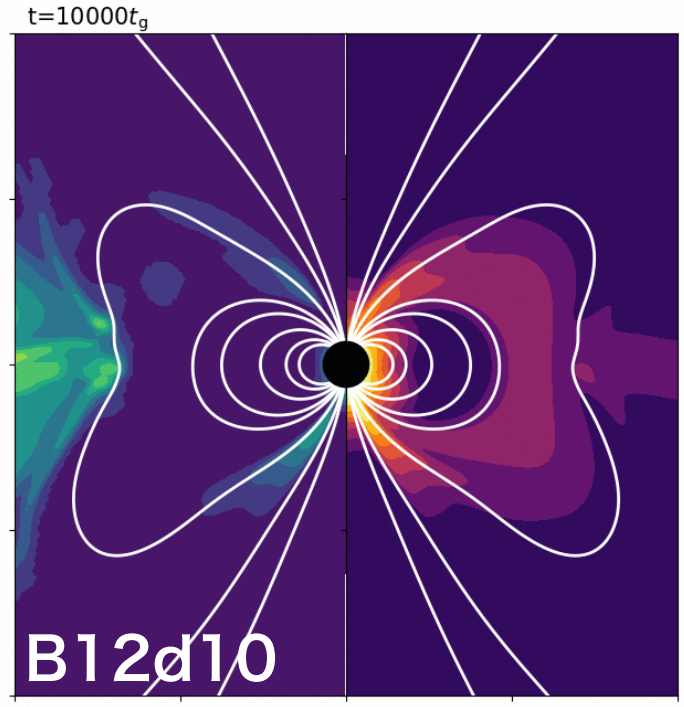
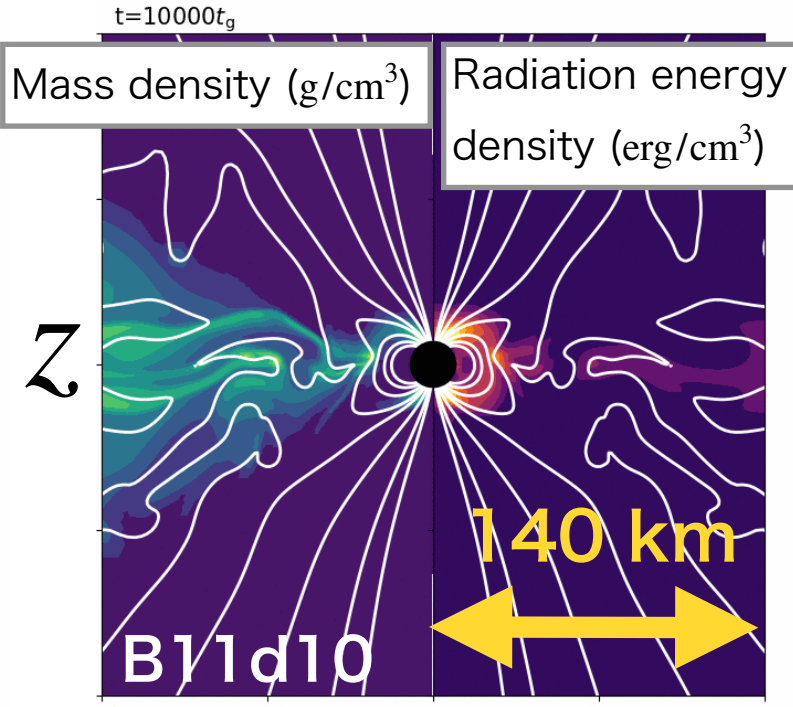
## Models

- B10d01 :  $\rho_0 = 0.1 \text{ g cm}^{-3}$ ,  $B_{\text{NS}} = 10^{10} \text{ G}$  • B11d1 :  $\rho_0 = 1 \text{ g cm}^{-3}$ ,  $B_{\text{NS}} = 10^{11} \text{ G}$
- B11d10 :  $\rho_0 = 10 \text{ g cm}^{-3}$ ,  $B_{\text{NS}} = 10^{11} \text{ G}$  • B12d10 :  $\rho_0 = 10 \text{ g cm}^{-3}$ ,  $B_{\text{NS}} = 10^{12} \text{ G}$

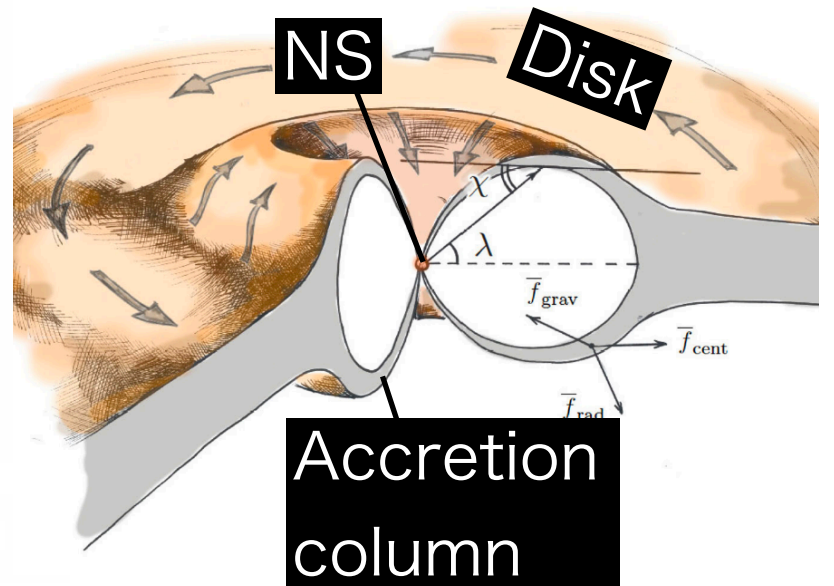
$\rho_0$  : maximum density of the initial torus ,  $B_{\text{NS}}$  : magnetic fields strength at NS surface

# Magnetospheric radius

$\rho_0 = 10 \text{ g cm}^{-3}$   
 $\rho_0 = 1 \text{ g cm}^{-3}$   
 Maximum density of initial torus  
 (corresponding to mass accretion rate)



Three-dimensional image of axisymmetric accretion flows  
 Mushtukov+2017

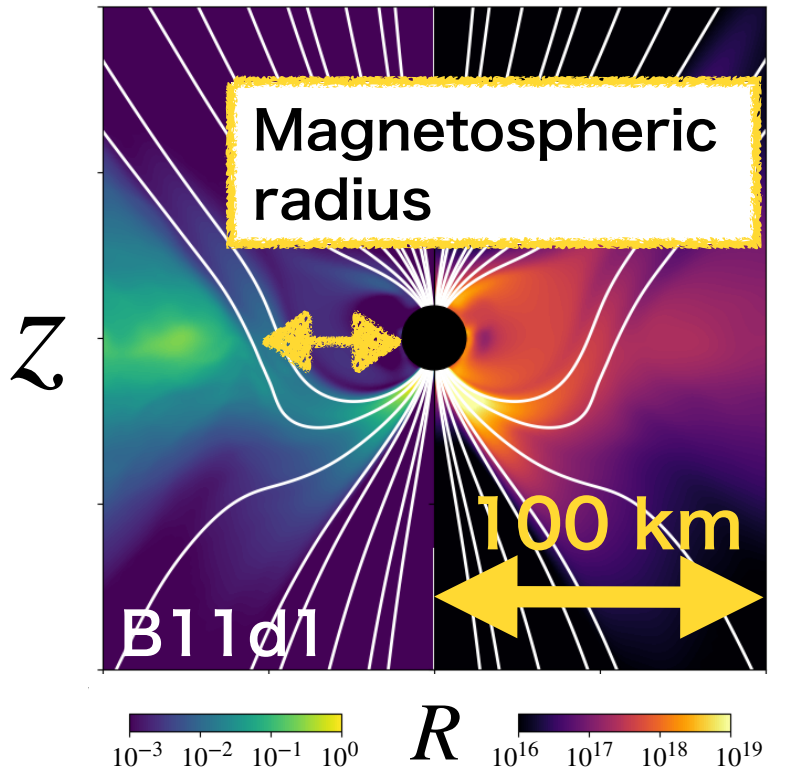
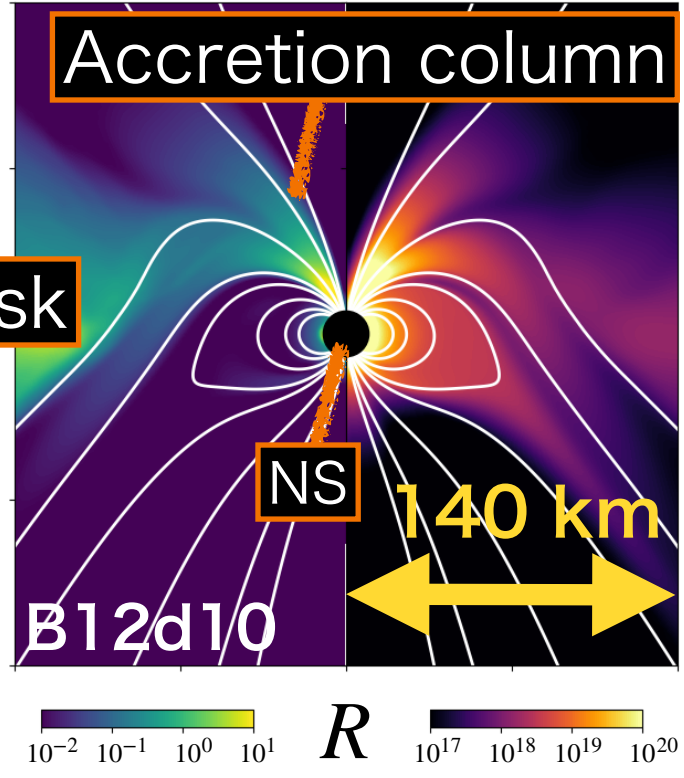
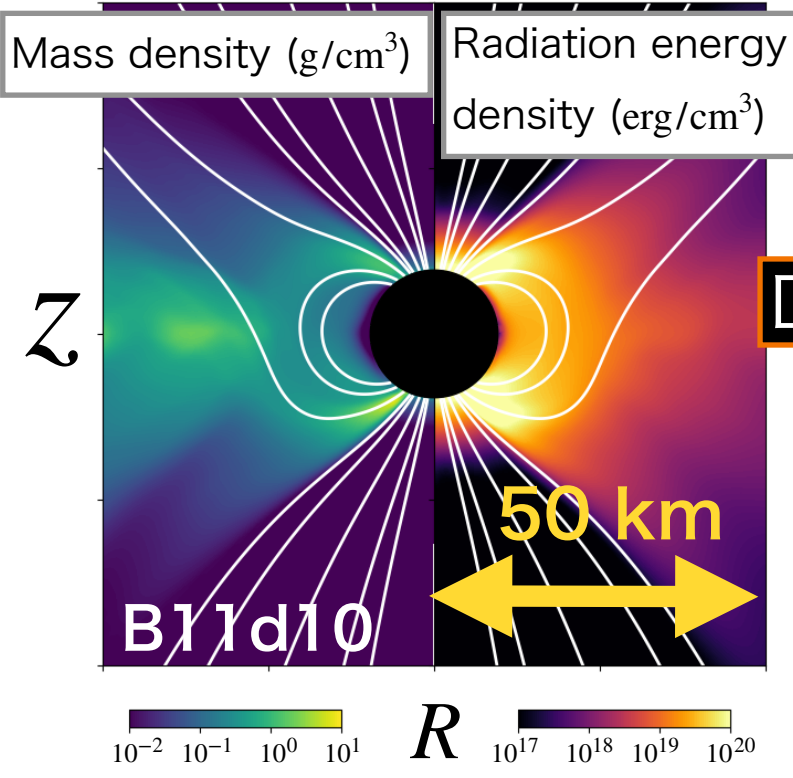


- The accretion disk is truncated by dipole field of the NS.
- Magnetospheric radius becomes large for the case of low accretion rate or high  $B_{NS}$ .
- If the the magnetospheric radius is large, the accretion column forms around either the north pole or south pole.

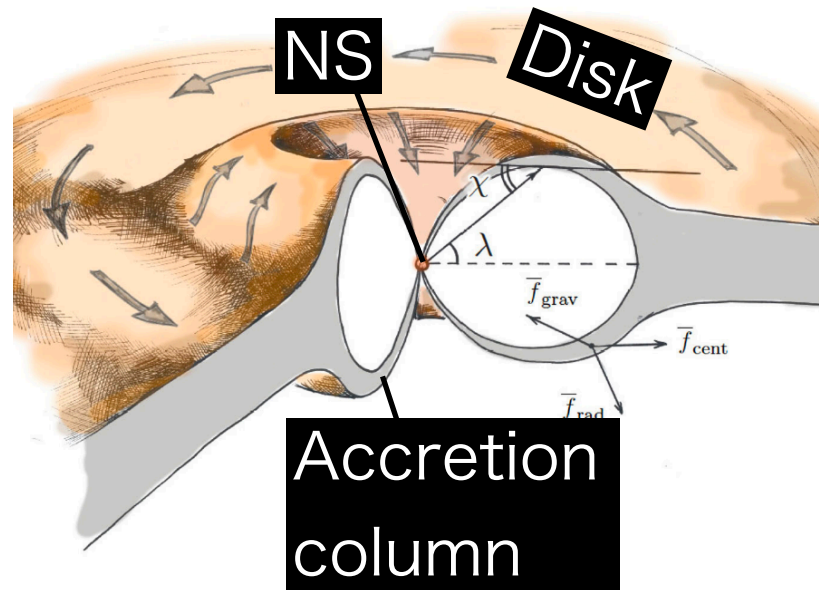
Magnetic field at NS surface  
 $10^{11} \text{ G}$        $10^{12} \text{ G}$

# Magnetospheric radius

$\rho_0 = 10 \text{ g cm}^{-3}$   
 $\rho_0 = 1 \text{ g cm}^{-3}$   
 Maximum density of initial torus  
 (corresponding to mass accretion rate)



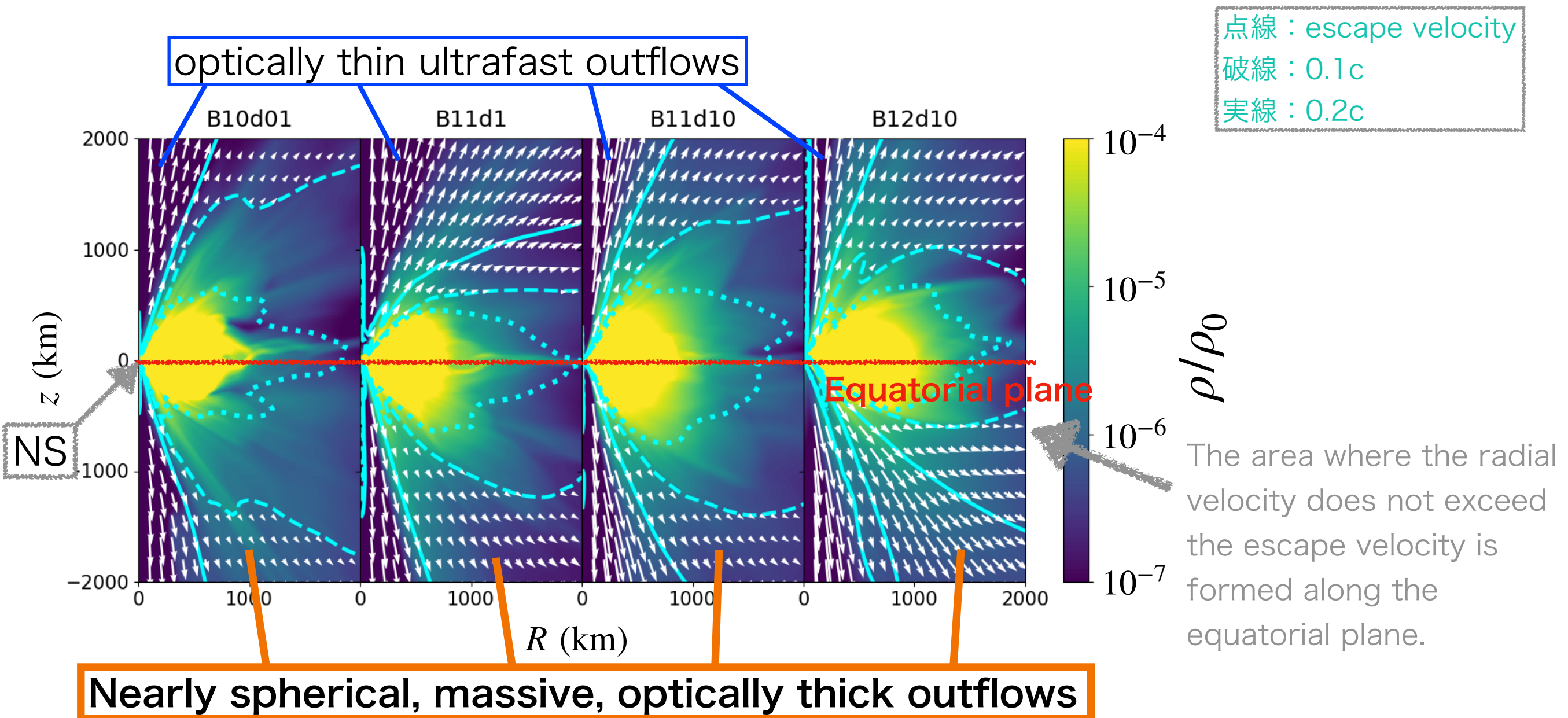
Three-dimensional image of axisymmetric accretion flows  
Mushtukov+2017



- The accretion disk is truncated by dipole field of the NS.
- Magnetospheric radius becomes large for the case of low accretion rate or high  $B_{NS}$
- If the the magnetospheric radius is large, it is difficult for accretion columns to form on both magnetic poles.

Magnetic field at NS surface  
 $10^{11} \text{ G}$   $10^{12} \text{ G}$

# Outflows driven by supercritical accretion



Resulting velocities are consistent with observed velocities (0.1c-0.2c).

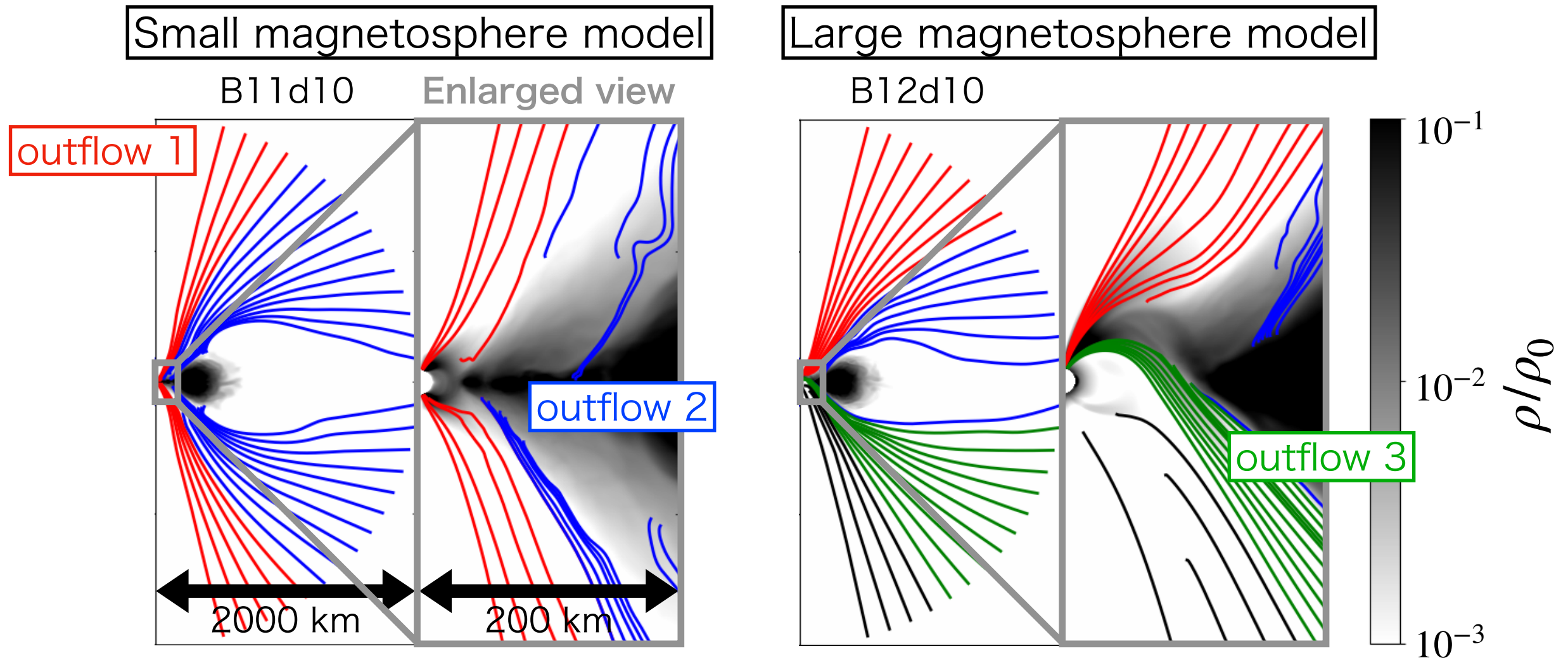
We investigate optically thick outflows in more detail, and it is revealed that **3 types of optically thick outflows are formed.**

# 3 types of optically thick outflows

The stream lines indicate optically thick outflows.

The difference in colors of the stream lines represents the difference in driven mechanisms.

Next slide



Stream lines of **outflow 1** and **outflow 3** are connected with an accretion column. **Outflow 2** is launched from the accretion disk.

We investigate driven mechanisms of 3 types of outflows.

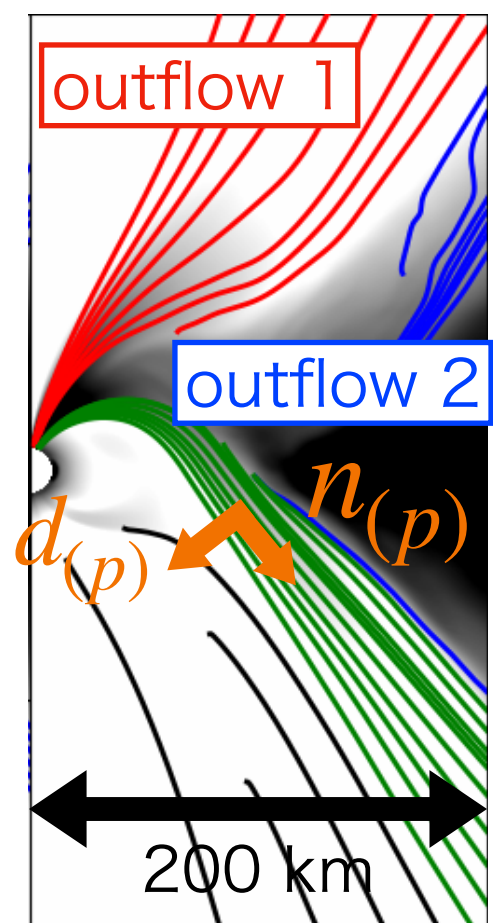
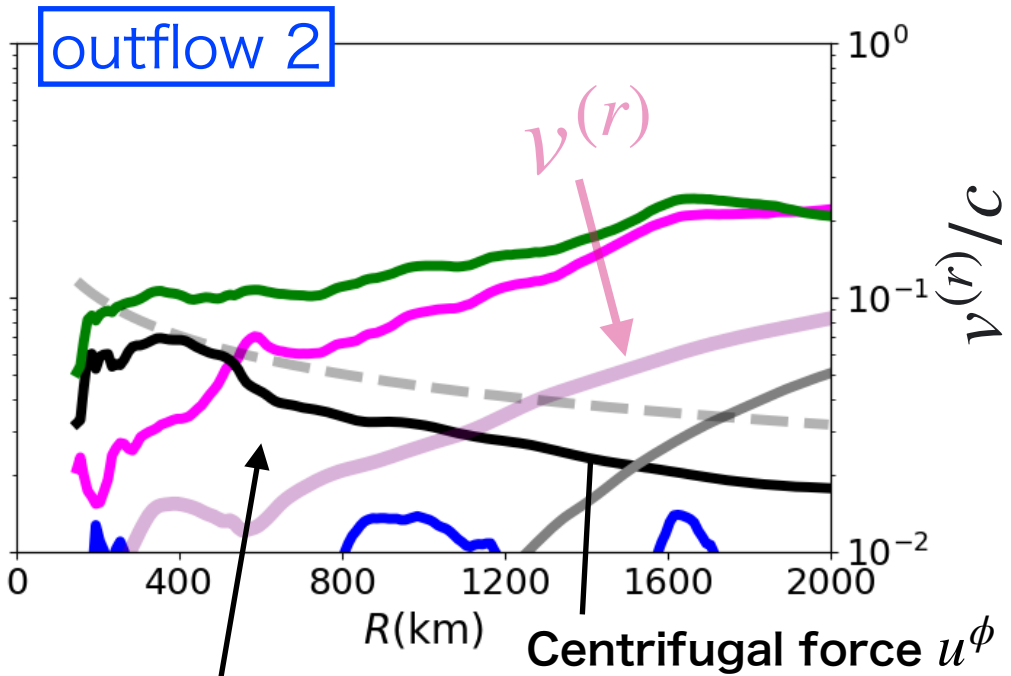
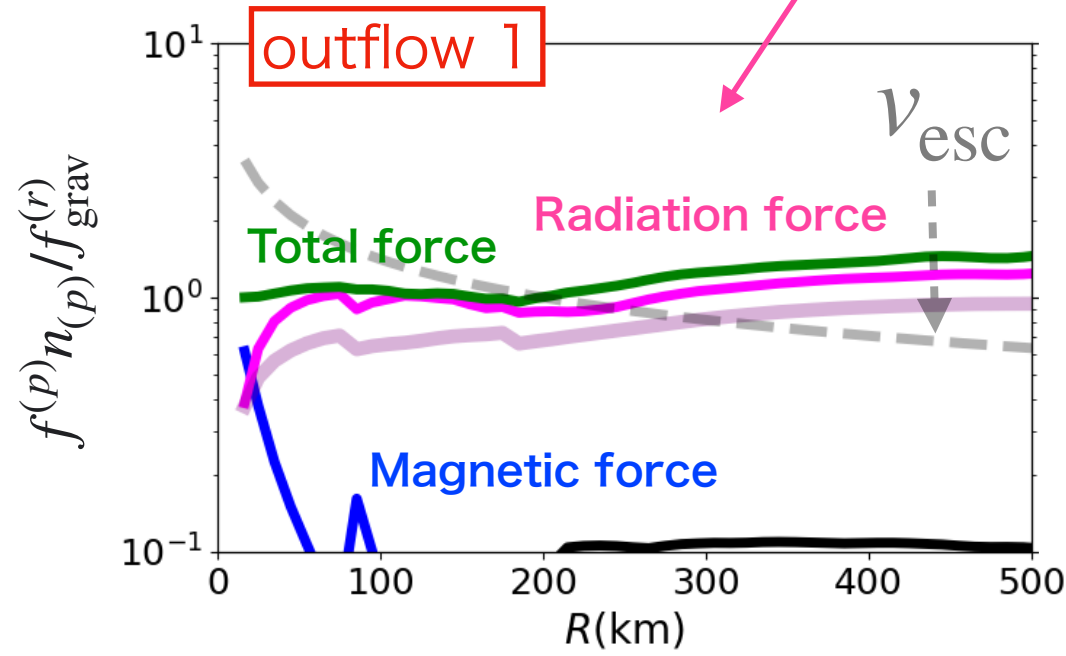
# Driven mechanisms of outflow 1 and 2

We calculate radiation forces, magnetic forces and centrifugal forces.

$n_{(p)}$  : unit vector along the stream lines  
 $d_{(p)}$  : unit vector perpendicular to the stream lines

the averaged value for stream lines of each outflows

Radiation force is dominant in the outflow 1.



Centrifugal force for  $u^\phi$  effectively works as well as radiation force

Outflow 1 : radiation force driven

Outflow 2 : radiation force + centrifugal force driven

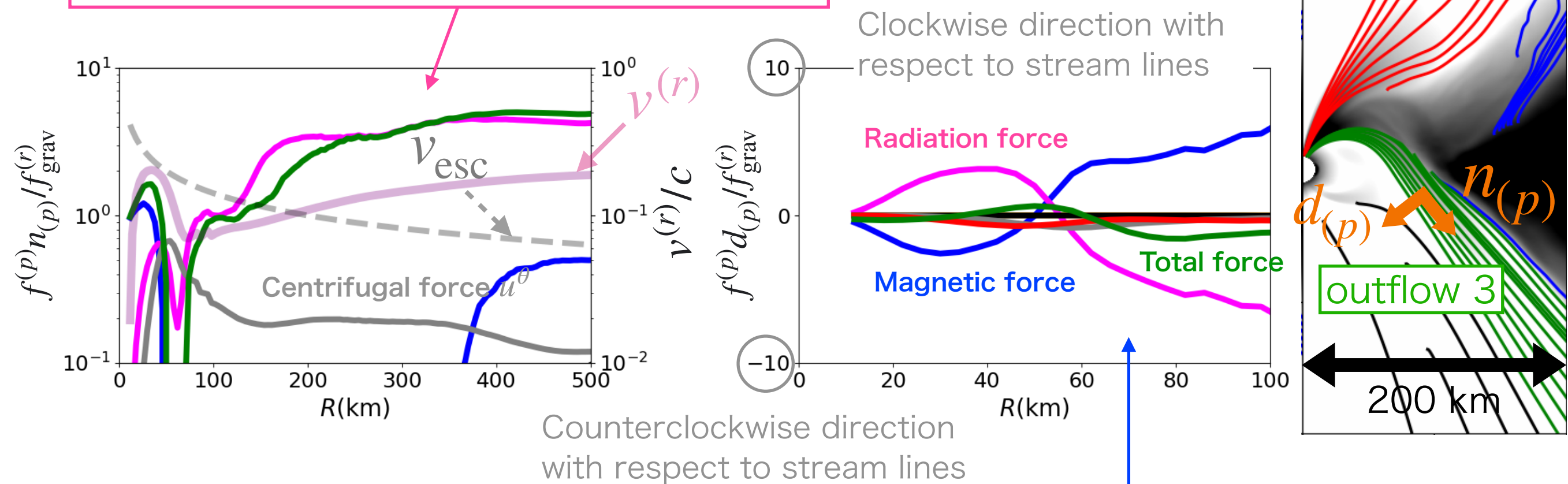
# Driven mechanisms of outflow 3

We calculate radiation forces, magnetic forces and centrifugal forces.

$n_{(p)}$  : unit vector along the stream lines  
 $d_{(p)}$  : unit vector perpendicular to the stream lines

the averaged value for stream lines of each outflows

Radiation force is dominant in  $r > 40$  km.

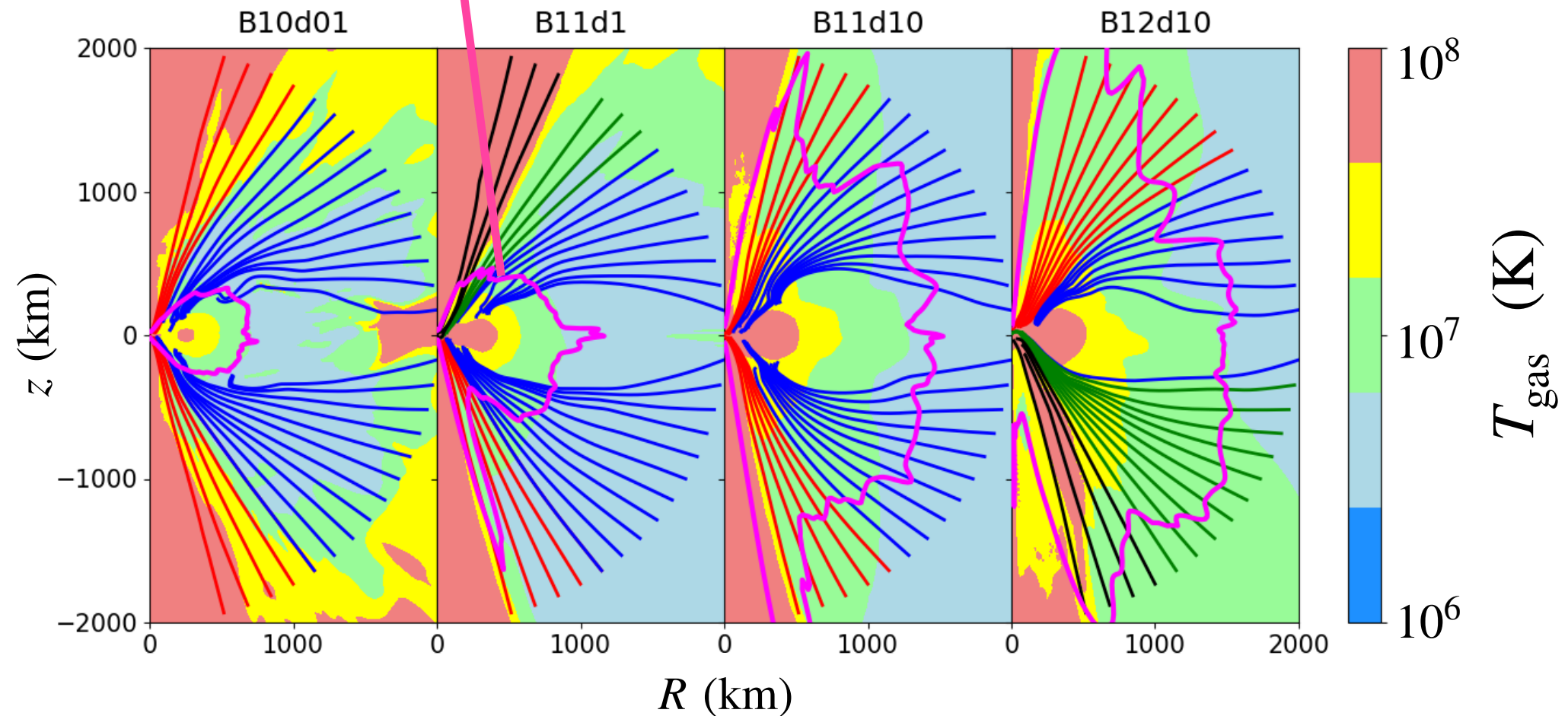


Magnetic forces support the accretion column ( $r < 50$  km) and change the outflowing direction of outflow 3 ( $r > 50$  km).

**Outflow 3** is mainly driven by radiation forces, and magnetic forces effectively work to change the outflowing direction.

# Photospheres and outflow temperatures

Effective Photosphere (radial direction)  
Radiation outside this line may be observed



Low ← **Mass accretion rate** → High

The higher mass accretion rate models, the larger effective photosphere is formed.

**Three types of optically thick outflows form effective photospheres above.**

# Comparison with Swift J0243.6+6124

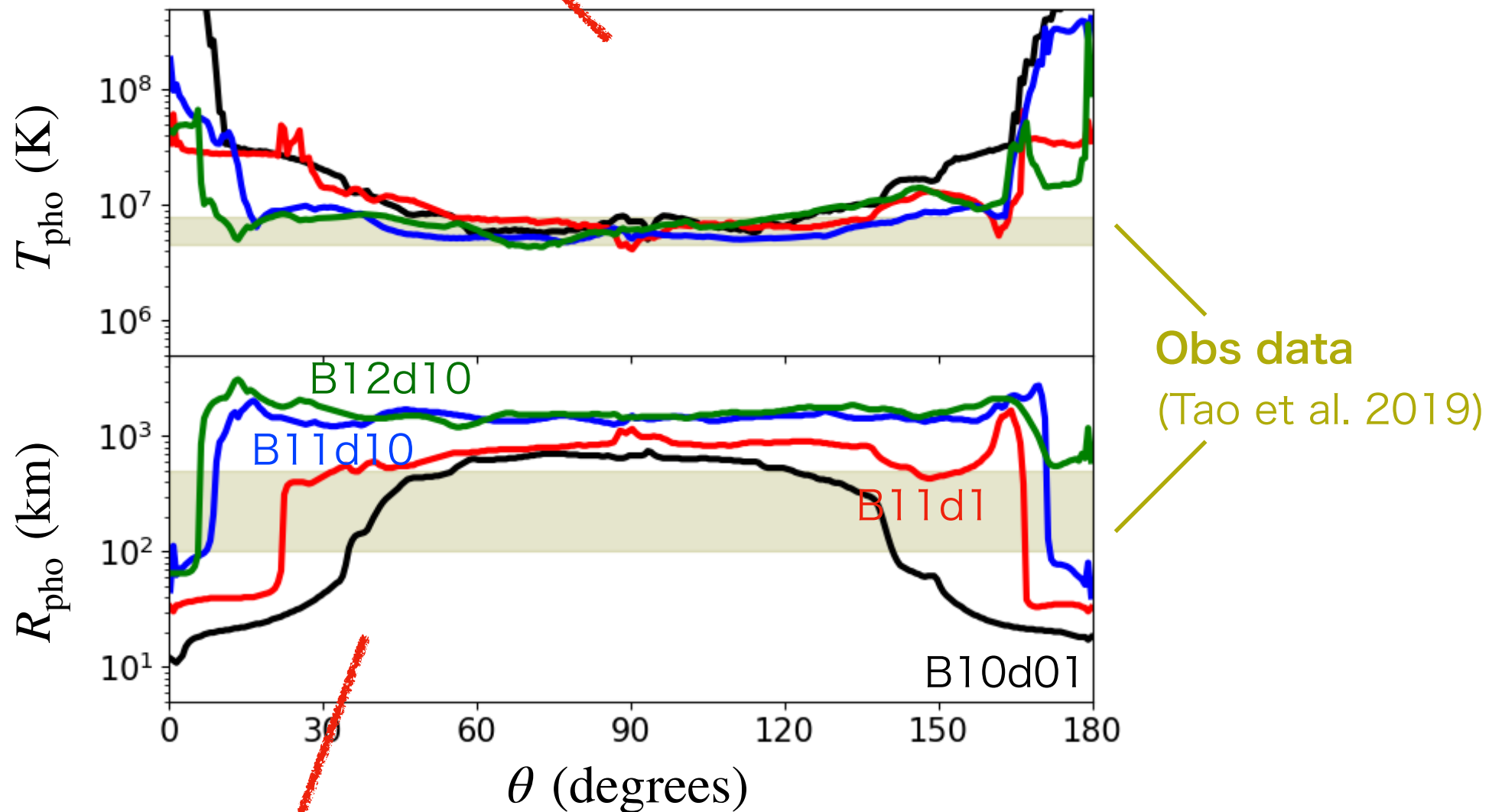
We estimate the blackbody temperature and the blackbody radius using effective photospheres.

Outflow temperatures obtained in our simulations are consistent with the observed blackbody temperature.

$$T_{\text{pho}} \equiv T_{\text{gas}}(r = R_{\text{pho}})$$

$R_{\text{pho}}$  : radius of effective photosphere

Roughly estimated values of the blackbody radius



$R_{\text{pho}}$  of model B10d01 in  $40^\circ \lesssim \theta \lesssim 60^\circ$  or  $120^\circ \lesssim \theta \lesssim 140^\circ$  (which is originated from outflow 2) are consistent with the observed blackbody radius.

# Summary

We performed ① **General-Relativistic radiative transfer simulations** and ② **General-Relativistic Radiation MHD simulations** of supercritical accretion flows onto the magnetized neutron stars.

① **Resulting pulse profiles are consistent with observed data in ULX pulsars**

② **The resulting outflow velocity, temperature and blackbody radius are consistent with the observed data in Swift J0243.6+6124.**

**Our present study supports the hypothesis that the ULX Pulsars are powered by the super-critical column accretion on to magnetized NSs.**

See Inoue et al. 2020 for ① in detail

General-Relativistic Radiation MHD simulations (②)

**3 types of optically thick outflows exist :**

**Outflowing matter comes from both the disk and the accretion columns**

Outflow 1 (launched from the column) : radiation force driven

Outflow 2 (launched from the disk) : radiation force + centrifugal force driven

Outflow 3 (launched from the column) : radiation force driven

# Future works

**In this study, the magnetic field of the NS is assumed to be the dipole field.**

How much do pulse profiles, accretion flows and outflows depend on the configuration of the magnetic field of the NS?

**Is it possible to explain the radiation spectrum in ULXs or ULX Pulsars with present models?**

Radiative post-processing is required to obtain more detailed information on the emerging radiation spectrum.

**We need to perform 3-dimensional non-axisymmetric simulations in order to calculate the pulse profile.**

Non-axisymmetric accretion flows on to magnetized NSs are important in ULX Pulsars.